



Contents lists available at ScienceDirect

## Journal of Controlled Release

journal homepage: [www.elsevier.com/locate/jconrel](http://www.elsevier.com/locate/jconrel)

# Design of experiments in the optimization of nanoparticle-based drug delivery systems

Riccardo Rampado<sup>a,b,c,d</sup>, Dan Peer<sup>a,b,c,d,\*</sup>

<sup>a</sup> Laboratory of Precision Nanomedicine, Shmunis School of Biomedicine and Cancer, Research, George S. Wise Faculty of Life Sciences, Tel Aviv University, Tel Aviv, Israel

<sup>b</sup> Department of Materials Sciences and Engineering, Iby and Aladar Fleischman Faculty of Engineering, Tel Aviv University, Tel Aviv, Israel

<sup>c</sup> Center for Nanoscience and Nanotechnology, Tel Aviv University, Tel Aviv, Israel

<sup>d</sup> Cancer Biology Research Center, Tel Aviv University, Tel Aviv, Israel

## ARTICLE INFO

## Keywords:

Design of Experiment  
Optimization  
Screening  
Drug delivery  
Nanomedicine  
Nanoparticles

## ABSTRACT

Design of experiment (DoE) is a powerful statistical technique used for variable screening and optimization. It is based on the simultaneous variation of multiple factors with the objective of finding the configuration of parameters that optimizes one or more outputs of interest, while using the minimal number of experimental runs required for testing, resulting very cost and time-efficient. Despite the high potential offered by this approach for innovation and process optimization, DoE is still only marginally applied in the field of nanomedicine and often its rationale application and analysis result is difficult to grasp by many. In this review, we discuss some of the latest applications of DoE in the formulation of nanovectors used for drug delivery across many different applications. First, we introduce general principles of DoE to the reader, which are indispensable to understand the works we report. Then, we give particular attention to the process variables, the specific designs, and the readouts used for process analysis and optimization for different classes of nanovectors. Finally, we try to delve into the current shortcomings of DoE application and possible future directions that could be employed to further improve the information that can be derived from this approach.

## 1. Introduction

The development of robust protocols and the establishment of a products are the essential building blocks upon which scientists advance knowledge and technology in any field of inquiry. This includes the field of nanomedicine. In particular, the creation of nanoparticle-based drug

delivery systems (DDSs) involves many different experimental conditions that could influence the outcomes and that largely depend on the specific material in study.

Any unknown process can be thought of as a “black box” in which the operator introduces materials and chooses specific settings. The process returns some measurable outputs (Fig. 1A). Thus, process optimization

**Abbreviations:** AI, artificial intelligence; ASO, antisense oligonucleotide; BBB, blood brain barrier; BBD, Box-Behnken design; CAP, capecitabine; CAR, carvedilol; CCCD, circumscribed central composite designs; CCD, central composite design; CCI, cell concentration at infection; CIL, cilnidipine; CPP, critical process parameter; CQA, critical quality attribute; CRC, colorectal cancer; Cs-A, cyclosporine A; DTX, docetaxel; DDS, drug delivery system; DoE, Design of experiment; EE, encapsulation efficiency; eGFP, enhanced green fluorescent protein; EM, eprosartan mesylate; FCCD, face centered central composite design; FMEA, Failure Mode and Effects Analysis; FMT, fluorometholone; FRR, flow rate ratio; GA, glutaraldehyde; ICCD, inscribed central composite design; FFD, full factorial design; FrFD, fractional factorial design; hSET-1, human SET-1; LAM, lamotrigine; LNPs, lipid nanoparticles; LPHNPs, lipid-polymer hybrid nanoparticles; Luc, luciferase; MD, mixture design; MOI, multiplicity of infection; MTX, methotrexate; N-Ac, N-acetylcysteine; NF, nuisance factor; NP, nanoparticle; NSAID, non-steroidal anti-inflammatory drugs; PDI, polydispersity index; PLGA, poly lactic-co-glycolic acid; PS, particles size; PTX, paclitaxel; PVA, polyvinyl alcohol; QbD, quality by design; QTPP, Quality Target Product Profile; RIF, rifampicin; RLZ, Riluzole; RPM, risk priority number; RSM, response-surface method; RU, rutin; SAN, self-assembling nano-carriers; saRNA, self-amplifying mRNA; S<sub>mix</sub>, Surfactant mixture; SNEDDS, self-nano-emulsifying drug delivery systems; SOP, standard operating procedure; STPP, sodium tripolyphosphate; TA, tartaric acid; TFR, total flow rate; TMC, trimethylchitosin; TOH, and time of harvest; VLPs, virus-like particles; ZNP, zein NPs; ZP, zeta potential.

\* Corresponding author at: Laboratory of Precision Nanomedicine, Shmunis School of Biomedicine and Cancer, Research, George S. Wise Faculty of Life Sciences, Tel Aviv University, Tel Aviv, Israel.

E-mail address: [peer@tauex.tau.ac.il](mailto:peer@tauex.tau.ac.il) (D. Peer).

<https://doi.org/10.1016/j.jconrel.2023.05.001>

Received 26 March 2023; Received in revised form 28 April 2023; Accepted 1 May 2023

Available online 12 May 2023

0168-3659/© 2023 Elsevier B.V. All rights reserved.

requires both understanding which settings (or parameters or variables) are relevant, and among these, select the best level of each to achieve a desired output. To achieve this, it is necessary to correlate the variables with the outcome features (Fig. 1B). When trying to optimize the features of these nanovectors, researchers are presented with the daunting task of understanding the significance and effect of many experimental factors in the process output. This hurdle induces scientists to use two main approaches.

The first one is a trial-and-error strategy, in which each variable is tuned singularly, selecting the best outcomes before optimizing the next one (Fig. 2B). This approach requires a limited number of experiments and can lead to good results. However, this strategy presents intrinsic limitations. Firstly, it is not possible to understand if some variables have more leverage than others, and no information is acquired on the possible synergistic or antagonistic effects of multiple variables interactions. Secondly, the final nanovectors may not be the best possible ones in the considered experimental range, but just a “local optimization” that is derived from the narrow scope of the screening.

The opposite approach to trial and error consists a complete screening of all the conditions in the selected experimental range (Fig. 1C). This strategy allows to acquire complete knowledge on the process. However, it can require a very high number of experiments to optimize even a handful of experimental factors, and becomes exponentially more expensive to perform when increasing the number of considered parameters and their different levels. This can require a very high amount of resources and workforce that can outweigh the benefits deriving from an optimal outcome.

Design of Experiments (DoE) tries to bridge the gap between these two opposite approaches (Table 1). DoE is a statistical methodology based on the simultaneous tuning of experimental parameters. It allows to create an optimal set of experiments that provides the maximal amount of information on the process, depending on the objective of the study. Thus, DoE allows to compromise some level on information to significantly reduce the time and resources allocated to the understanding and optimization of any given process (Fig. 2D). This powerful tool can be used efficiently in research, when the aim is to quickly select only variables with a significant effect on the final outcomes and to optimize them to achieve the desired results. This is especially relevant in research groups with limited workforce and resources.

Despite its high potential, DoE is often overlooked outside of the engineering field, and its effective application and correct interpretation can result challenging to non-specialists due to the complex mathematical theory it involves. This is demonstrated the very small percentage of articles published in PubMed that apply DoE in their studies. Although, this percentage increased in the last twenty years, it still represents only 2% of the overall publications on nanomedicine (Fig. 3).

In this review, we offer a practical guide on the use of DoE to optimize nanovectors for drug delivery. We will focus on elucidating DoE terminology, discuss recent and most relevant examples of DoE application to nanomedicine, and give some practical advice on how to apply

DoE to any nanoparticle study, including future directions. Despite not being an extensive discussion on DoE, we believe this article can give the basic tools to understand DoE to a wider public, and communicate the potential it holds for discovery and innovation, and give a primer on how to implement it, together with possible sources for more in depth DoE exploration.

## 2. Key concepts of DoE

In this section, we will present some key concepts commonly applied to DoE, and their rationale, in glossary form to facilitate their consultation. These summary definitions are not exhaustive on the matter, and we point the reader to *ad hoc* manuals for in-depth discussion of DoE [1,2] and of the mathematical theory behind the generation of different designs. Design generation and subsequent analysis is commonly performed by specialized softwares, most of which we report for each analyzed publication in Tables 4 to 8.

Critical Process Parameters (CPPs): a CPP represents any factor or setting that is considered for the performance of an experiment or the analysis of a process. CPPs can be quantitative (e.g., formulation temperature, concentration of reagents, mechanical stress, flow rates in microfluidics systems), can be qualitative (e.g., using different lipids or polymers with different features in the formulations) or can be a mixture component (e.g., a molar ratio of the different NPs components). CPPs can be controlled or not. If a CPP cannot be fixed by the operator (e.g., batch of a chemical, environmental conditions of the laboratory), it is considered a nuisance or noise factor (NF). The range of CPP values defines the experimental space of the study.

Critical Quality Attributes (CQAs): CQAs are any measured process output. CQAs can also be quantitative (e.g., NPs size, size distribution, zeta potential (ZP), loading efficiency, payload release profile) or qualitative (e.g., NPs shape, or acceptability criteria). In some instances, the CQAs are grouped as Quality Target Product Profile (QTPP).

Design: a design is a set of different experimental runs. Each run can be represented as a point in a multidimensional space, in which each dimension is represented by a CPP (independent variable) or by a CQA (dependent variable).

Model: a model is the mathematical equation that correlates CPPs to each CQA. This interpolation can be performed using a variety of different regression methods. Each correlation is represented by a polynomial equation in which every CQA is a CPPs sum, each CPP exerting its effect through a coefficient. The equation can include linear, quadratic or cubic effects of each CPP, or the interactions between two or more CPPs. The complexity of these equations is increases with the number of experimental runs in the design that allow to elucidate more information.

Two- or multi-factor interactions: Two or more CPPs changing simultaneously can have effects that are higher or lower than the sum of single CPPs. This constitute synergistic or antagonistic multi-factor effects.

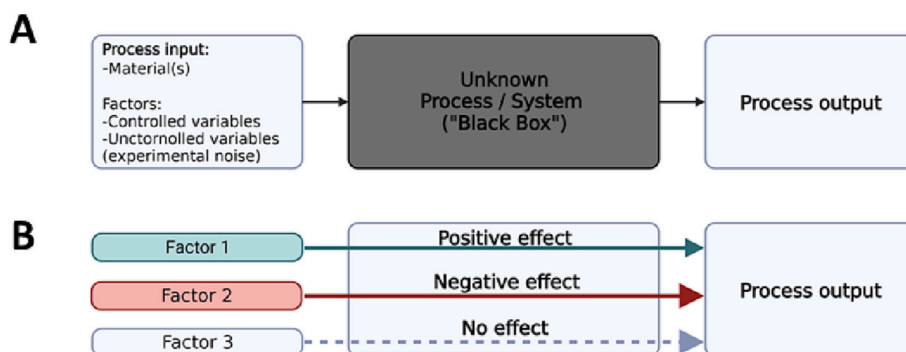
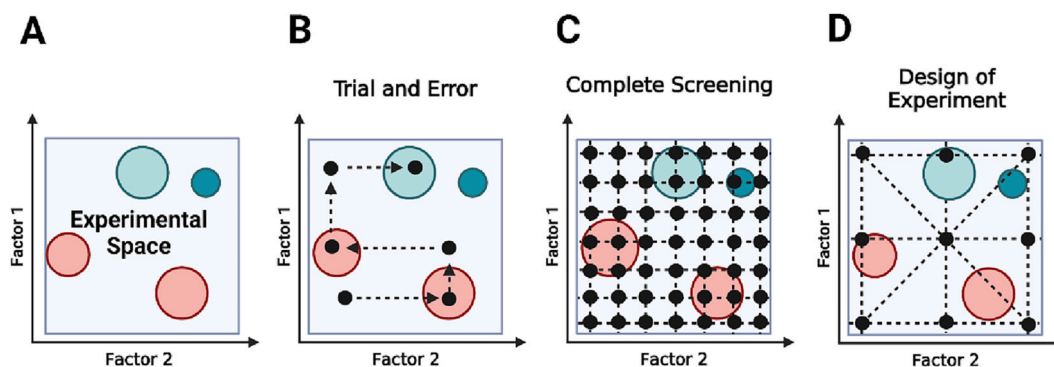


Fig. 1. Schematic representation of processes or systems as black box (A) and the different influences of factors in the final output (B).



**Fig. 2.** (A) Schematic representation of a two-dimensional experimental space defined by two quantitative experimental factors. The red spots on the surface represent undesirable outputs ranges, while green spots desirable outputs ranges, with the dark green circle representing the optimal factors combination. Black dots represent an experimental run defined by specific factorial values as coordinates. (B) Schematic representation of a trial and error experimental approach, complete screening (C), and a hypothetical design of experiment (S). This image was made using [Biorender.com](https://www.biorender.com). (For interpretation of the references to colour in this figure legend, the reader is referred to the web version of this article.)

**Table 1**

Direct comparison of the potential advantages and pitfalls when using a trial-and-error, complete screening, or DoE-based approach.

	Trial and Error	Complete Screening	DoE
Single Factor Effects Analysis	Very limited	Feasible	Feasible
Multiple Factors Effects Analysis	Not feasible	Feasible	Feasible if desired
Maximal Optimization	Not feasible	Feasible	Feasible
Overall Information on the process	Minimal	Feasible	Can be decided by design
Number of Experiments Required	Low	Very high	Minimized by design

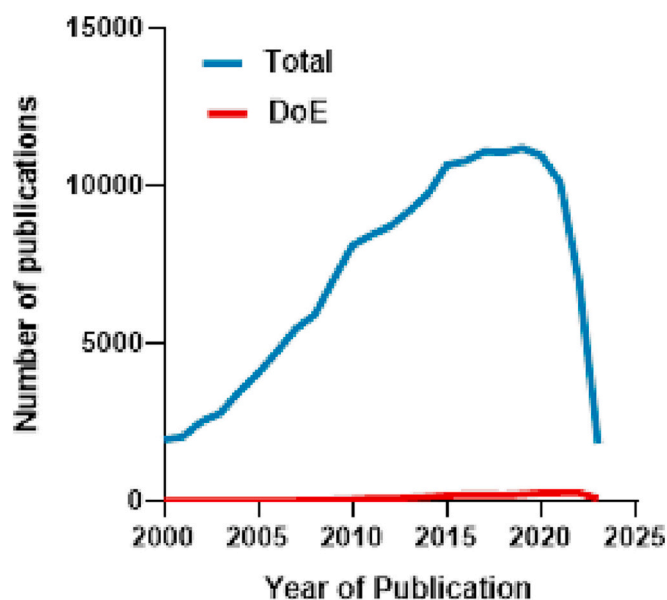


**Fig. 3.** Number of Publications present on PubMed regarding nanomedicine and drug delivery systems from 2000 to 2023 (Blue line), Number of these publications that include DoE (red line). (For interpretation of the references to colour in this figure legend, the reader is referred to the web version of this article.)

**Center point:** a center point is an experimental run located at the center of the experimental space and localized by intermediate values of all CPPs. If multiple center points are present, they are distributed

homogeneously within experimental set. The center points are useful to check for process stability, since unstable center point values are symptom of a process with inconsistent results. Center points also allow to see if the CPP to CQAs relations across the experimental space are linear or not. This can suggest to create enhanced designs to account for nonlinear effects. Normally, RMS designs give the best performance when using 2 to 5 center points [1].

**Degrees of freedom:** This term indicates how many direct comparisons can be performed within a design. This is of critical importance to understand how much information can be elucidated from a number of experimental runs. A direct comparison is defined as two experimental runs that change only by one CPP value.

**Confounding and aliasing:** this term indicates the impossibility to understand which CPPs, and to what extent each CPP contributes to a CQA. This is critical in designs with few experimental runs that do not allow many direct comparisons. Each one of the cofounded CPP is defined as an alias. Understanding which factors can be confounded is paramount to prevent the erroneous interpretation of a model.

**Blocking:** When a design requires the parallel work of multiple operators, or the use of different material batches, there is a chance that these factors can affect the experimental results *per se*. Thus, blocking allows to separate the experimental set in homogeneous subsets to consider and reduce the effects of this experimental noise. Blocking can be performed by dividing the experimental runs into homogeneous groups, often using as sorting factor a high order interaction not studied. Thus, a high order interaction will be confounded with the blocking effect itself. When the blocking does not affect the confounding pattern of the design, it can be considered orthogonally blocked.

**Design resolution:** this term indicates the confounding pattern of a design. Specifically, in resolution III designs no main CPP is confounded with any other factor, but two factors' interactions can be confounded with main factors and with each other (Fig. 4A). Resolution IV designs do not have confounding among main factors and among main factors and two factors' interactions, however, interactions are confounded with each other (Fig. 4B). Resolution V designs have no confounding between main factors and two factors' interactions, but only among two factors interactions and higher interactions (Fig. 4C).

**Orthogonality:** this propriety indicates how independently each comparison can be performed. In an ideal condition, X factors are orthogonal if X-1 comparisons (or degrees of freedom) are present in the design.

**Randomization.** When performing a set of experiments, sometimes it is not possible to perform all the runs in parallel. This constraint dilates the time required to complete the set and can require the repeated use of instruments and materials. However, materials can degrade and instruments can wear out, shifting the results of the experiments during

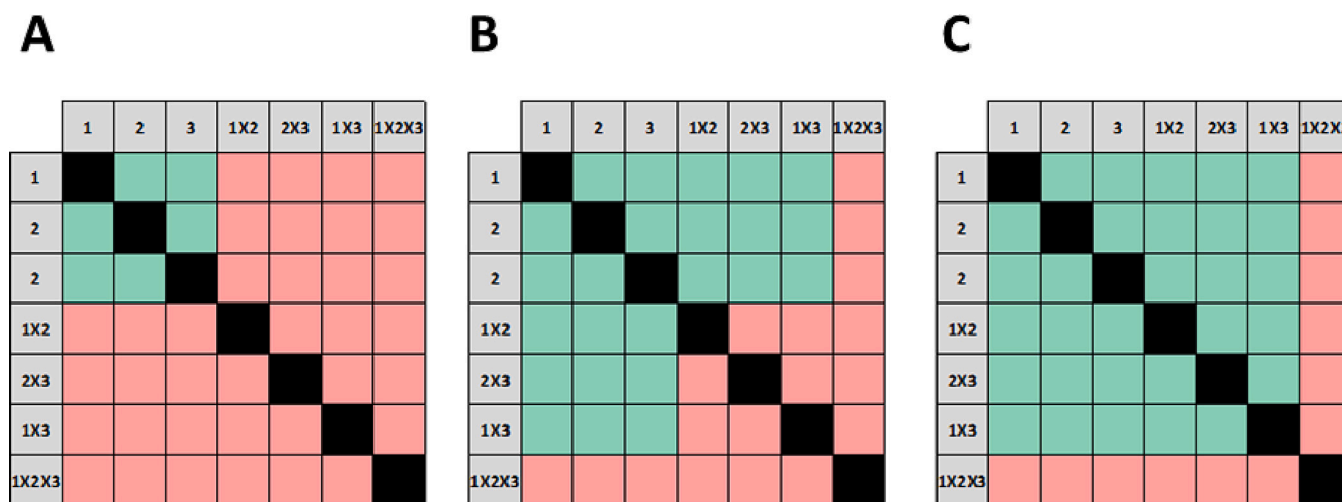


Fig. 4. Representation of the different levels of designs resolution III (A), resolution IV (B) and resolution V (C). The green area represents well-resolved single CPPs (1,2,3) and multiple factors effects, while the red area represents the confounded effects. (For interpretation of the references to colour in this figure legend, the reader is referred to the web version of this article.)

their execution. Randomization allows to perform the experiments in a casual order, leveling the effects caused by this shift.

Variance: variance defines the effect that CPPs can have on a CQA. When CPPs acquire values close to the experimental space outer boundaries, the variance increases since the difference between the boundary point and other points in the space is larger. *Vice versa*, variance lowers towards the center of the design.

Rotatability: this propriety refers to the variance profile of the predicted values across the experimental space. In a rotatable design the variability increases from the center of the space towards its boundaries, independently of the specific direction (Fig. 5).

Optimality: experimental designs are often limited by practical hurdles, such as the maximal number of runs, or the limited amounts of material available. Thus, many DoE softwares allow to apply optimization criteria to improve the design features, depending on its final aim. Two widely used approaches are the D-criterion and the I-criterion [3]. The D-criterion relates to the factor effects variance, while the I-criterion focuses on predictive precision. Specifically, the D-criterion improves the design ability to elucidate the effect of CPPs or interactions on the CQAs. It does this by organizing the experimental runs across many different and distant CPP values in the experimental space. However, D-optimal design can overlook non-linear factors' effects, and thus require design modifications. The I-optimality criterion instead improves the predictions accuracy offered by the final model. I-optimal designs involve more experimental runs in the experimental space center, thus minimizing the prediction variance in this location., However, variance

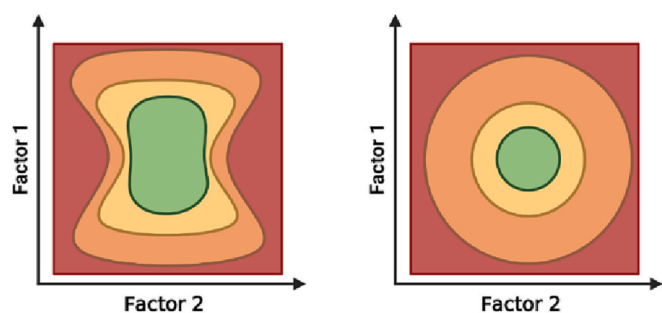


Fig. 5. Schematic representation of a two-dimensional design space variability defined by two quantitative experimental factors in a non-rotatable experimental space (left) and a rotatable space (right). This Figure was created using [Biornder.com](https://www.biornder.com).

becomes higher than D-optimal designs at the boundaries of the experimental range (Fig. 6). These two criteria are not mutually exclusive, since unconstrained designs such as full factorial design can be both D-optimal and I-optimal (see next section).

Desirability functions: these functions are normally defined for each CQA when setting up the experiment in *ad hoc* softwares. This approach allows to classify any outcome with a quantitative value for acceptability that ranges from 0% to 100%. The desirability functions can aim to achieve a specific CQA value or range of values, or maximize or minimize a CQA. Often multiple desirability functions are defined for multiple CQAs in a single process, and thus the software performs optimization by finding the highest desirability value achievable across all functions, and it interpolates the CPPs levels leading to this result. It

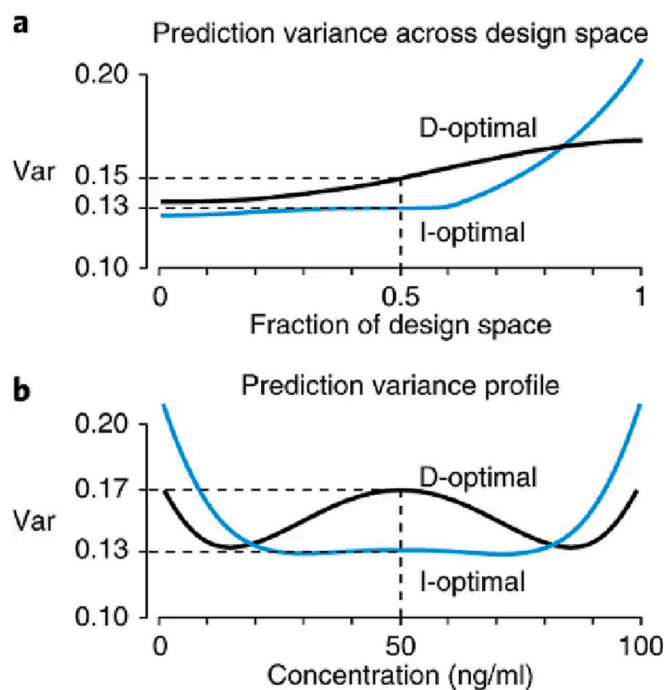


Fig. 6. Prediction variance of D-optimal and I-optimal experimental designs presented as fraction of experimental space (A), in which the center of the designs corresponds to the origin, and as actual trend across the levels of one experimental factor (*i.e.*, concentration, B). This image was taken from [3].

is important to note that sometimes the desirability functions can be contradictory, and therefore the software will find a compromise between them. This can lead to low global desirability values, and it might become necessary to remove or to reduce the importance of one of the contradicting CQAs.

**F-test and F-score:** F-test is a type of statistical analysis applied to DoE data, normally performed by ANOVA softwares. This test allows to elucidate statistically significant differences between multiple groups of data. This is performed by assigning to each data group an F score. F scores are calculated by dividing the variance between groups by the variance within each group. The more the groups are apart from each other and the narrower each group is, the higher the F score becomes and the more significant their difference becomes. The F-scores are normally correlated with *p*-values to indicate statistical significance. Thus, F-scores can be used to understand if the differences observed by a model are significant or are likely caused by noise.

### 3. DoE workflow

The first step when considering DoE is defining clearly the process to be studied. This includes a careful selection of the CPPs to be investigated and the CQAs that will be measured. The factors can be selected based on previous literature or data suggesting their relevance. It is essential to have a very fine control over the selected CPPs to minimize the experimental variability. An example of this is the preparation of stock aliquots of different reagents and chemicals used in the formulations beforehand. If relevant, factors interactions might be included in the design. It is also important consider potential experimental noise and plan all activities to reduce it (e.g., randomization, blocking). These uncontrolled variables should be accounted for and either removed or considered as NFs or noise (e.g., changes in environmental moisture and temperature, different material batches, different operators involved). Make sure the process is stable enough to perform, and if not, try to improve it before trying to apply a DoE that could give no results due to excessive variability. This can be established by performing a series of repeated formulations by different operators and over time.

In some instances, it might be useful to apply a process of Failure Mode and Effects Analysis (FMEA). The extensive discussion of this approach would go beyond the scope of this article since it is not strictly related to DoE, and detailed publications on the matter are available [4]. Very briefly, FMEA is a process in which all the potential failures in a process or product are identified, prioritized and are eliminated or minimized. This is performed by classifying each potential failure on the basis of a severity score (S, from 1 to 10, higher with increasing severity of the failure), occurrence effect (O, from 1 to 10, increasing with frequency), and ease of detection (D, from 1 to 10, increasing with difficulty of detection). Then, failures are ranked by calculating the risk priority number ( $RPN = S \times O \times D$ ). For each failure an adequate control is chosen and validated, as well as adequate actions to reduce or eliminate the possibility of failures occurring, starting from the ones with the highest RPN. Some authors also apply Ishikawa diagram (or “fishbone” diagram) to better visualize the different categories of CPPs and potential process pitfalls.

The CQAs should be accurately and precisely measured using robust instruments and techniques that need to be previously validated. In some softwares, it is possible to create a hierarchy of CQAs, defining the most important ones for the objective of the study. Of note, quantitative outcomes summarized by a numerical value (e.g., NPs size, loading/encapsulation efficiency (EE), percentage of release at defined times,  $IC_{50}$  values, circulation half-life after administration, reduction of disease burden *in vivo*) allow for better modeling of the results.

The objective of the study must be specified, as well as how much in depth it is desired to go in terms of understanding two-or multiple factors interactions.

The second step is the selection of a specific design. This step is critical because irreversibly defines the amount of information that can

be acquired, and this cannot be changed *in itinere* or after performing it. Selection of the design will be treated in more detail in the next section. It is important to consider the possibility of performing blocking and randomization. The general rule applied in this case is “when possible block, when not possible randomize”, referring to NFs or noise that can be controlled, or that change randomly. It is also possible to test different designs, different number of runs and different number of runs or center points to iteratively refine the design.

In the third step, the actual experiments are carried out. It is of particular importance to minimize the experimental variability by careful quality control and the establishment of standard operating procedures (SOPs) that harmonize the work performed by different operators. SOPs are normally written down as detailed protocols which include adequate controls and pitfalls (e.g. turbidity of the solutions in case of material degradation, adequate cleaning of the instruments and glassware before and after formulations). Furthermore, each operator must record any discrepancy or malfunction encountered during the runs.

The final step is data analysis. In this case as well, softwares are widely used to perform extensive data analysis, detecting which CPPs are relevant in defining the process variability and outcome, select the optimal factors settings according to the goals, and allow for the addition of new runs to improve the design further if desire. After modeling, it also possible to simulate results for any given CPPs levels within the experimental space that can also include artificially generated noise (e.g. Monte Carlo simulation of a large number of NPs formulations within a certain range of CPPs values to check for robustness of NPs size and size distribution). Data analysis will also be discussed in more detail in sections below.

It is often convenient to perform multiple studies iteratively. Specifically, it is common to first run a screening design to select only the relevant CPPs, and then perform a second smaller design using only these parameters for further optimization. Ultimately this approach is more economical and yields more accurate and robust information. The second design can consider only significant factors, thus allowing to perform less runs for the same amount of information, or it can enable more in-depth information with the same number of runs, with less aliases, higher resolution, and the possibility to explore factors interactions. Another option is reducing the experimental space to a smaller range of CPPs levels with the aim to find the more precisely the best conditions for optimization. A third option can be improving the process robustness, to ensure better reproducibility. The overall DoE workflow is summarized in Fig. 7.

### 4. How to choose a specific design for DoE

As discussed above, when considering applying DoE to the study of a process, the most critical point is the selection of a specific design. Thus, designs are chosen depending on the final aim of the operator. The main objectives normally are:

- **Comparison:** this objective considers multiple factors, but the main goal in this case is understanding the relevance of one main *a priori* factor under different conditions.
- **Screening:** This approach is widely used to select only CPPs that have a relevant effect on the process's outcomes and “screen out” the non-significant CPPs. This is especially useful as a first step to elucidate only the most relevant factors for further optimization, limiting the final number of runs required.
- **Response surface method (RSM):** this objective focuses on the modeling of interactions between CPPs and CQAs, creating a function that can be visualized as a multidimensional surface for each considered outcome, where the independent variables are the CPPs. This objective is used for process optimization, first finding a specific point or region on the surface with desirable CQAs and extrapolating a predicted optimal set of CPPs values that would lead to it. RSM can

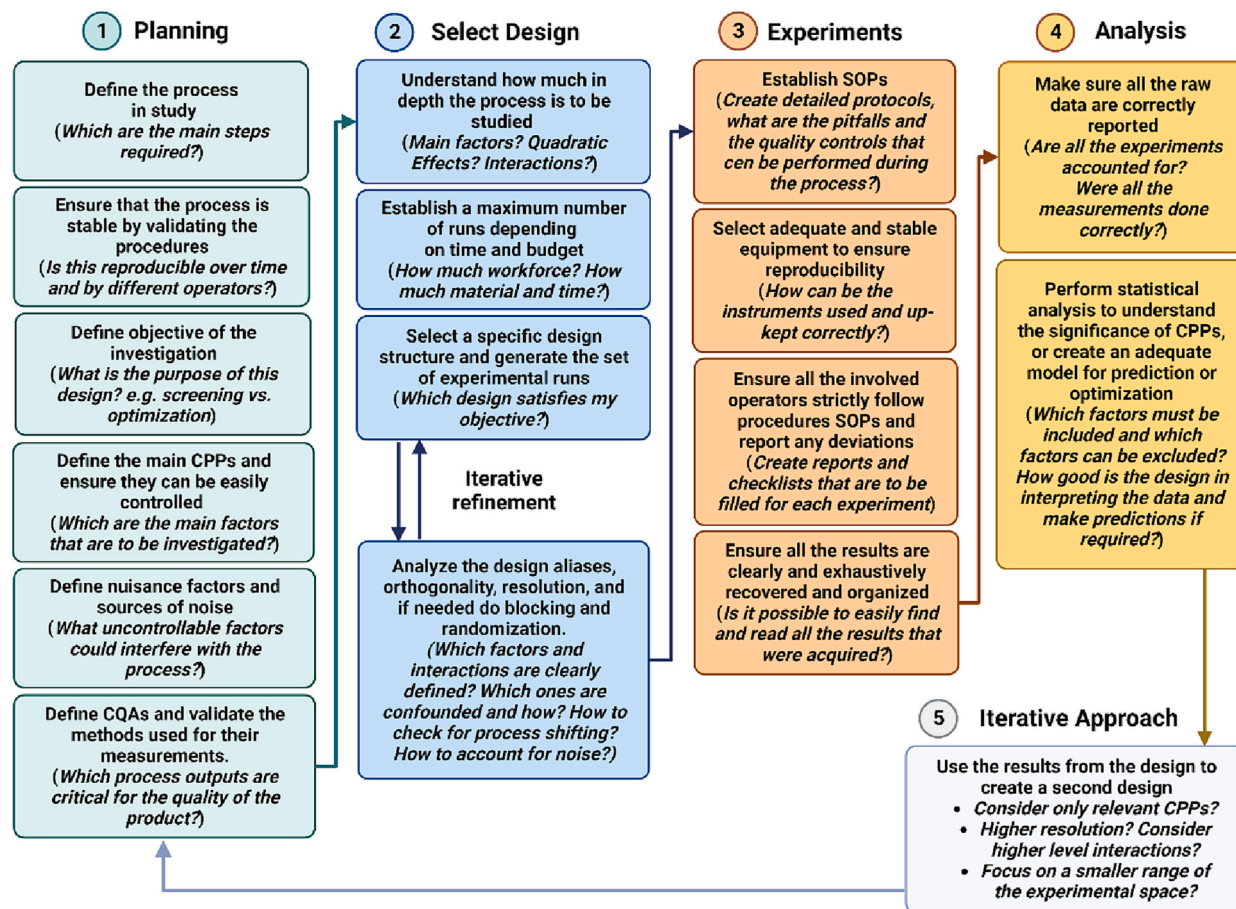


Fig. 7. summary of the general workflow used for the design of a DoE planning, setup, execution and analysis. This figure was created using Biorender.com.

also be used to improve the process robustness. In this case, the aim is to find “flat” regions of the surface with desirable outcomes, that would lead to the same acceptable results even by partially changing the factors, making the process less susceptible to CPPs shifts or to environmental conditions.

Other specific objectives for DoE designs include:

- Optimization of a mixture: this approach is often applied in chemistry. In this case the different factors are represented by different proportions of ingredients composing a mixture. These experiments are conceptually very different from most other designs, since when a single component proportion is changed, the others change accordingly. Thus, these factors are defined as “co-variate”. This feature is important to keep in mind because makes the contribution of a single factor very difficult to distinguish from the others unless it is removed from the mixture, preventing these experiments to be used as a screening approach. In this case the objective is always to find the best combination of proportions.
- Optimization of a regression: in this case, the main aim is to interpolate a function to correlate few continuous factors to an outcome.

However, designs are also chosen depending on the nature of the process and the number of CPPs in study and their potential levels. The choice of design should also carefully consider the number of experimental runs that are required and therefore the time, workforce and materials that define the budget of the overall study.

Table 2 gives the different types of designs summarized above and used in the literature. Table 3 summarizes the pros and cons of each design discussed in the following section. In depth discussion on the

Table 2

Summary table on which Designs can be selected depending on the Experimental goal and number of factors considered. This table was adapted by [1].

Number of factors	Comparison	Screening	Response surface
1	1-factor design (Preferably randomized)	NA	NA
2 to 4	Randomized Block Design	Full factorial or fractional factorial designs	Central composite designs or Box-Behnken
5 or more	Randomized Block Design	Fractional factorial or Packett-Burman designs	Apply a screening design first to reduce the overall factors

mathematical proprieties of each design is left to excellent *ad hoc* publications on the matter [1,5,6]

### 5. Specific types of designs

- 1-factor design: In this case, one single factor with different levels is considered. This is the most elementary design since it works only on one axis, keeping all the conditions constant except for the factor in study (Fig. 8A). The only modification that can be applied to this design is simple randomization to avoid experimental bias due to process shifting.
- Randomized block design (RBD): This design also considers a single factor in study. However, in this case, NFs are considered (Fig. 8B). NFs are not included to understand their specific effect on the process

**Table 3**  
Summary of the pros and cons of the different designs discussed in Section 5.

Design	Pros	Cons
FFDs	No confounding / aliasing among CPPs and factor interactions (high number of degrees of freedom).	Can require a very high number of runs with numerous CPPs in study. Every CPP has only a maximum and minimum value, not allowing to model quadratic effects. High order interactions often become confounded / aliased.
FrFDs	Requires only a fraction of runs of the corresponding FFD.	Every CPP only has a maximum and minimum value, not allowing to model quadratic effects.
PBDs	Useful to screen a high number of CPPs at once.	Has very low resolution and allows only to estimate main factors effects. Require careful consideration of which CPP subtype to employ.
CCDs	Every CPP has more than two values, can estimate quadratic effects and high order interactions, and thus can be used for RSM analysis.	Can require a high number of runs due to the multiple levels of each CPP.
BBDs	Normally requires a lower number of runs than other RSM designs.	There is no information on the process at the corner boundaries of the experimental space.
Taguchi arrays	Allows to account for NFs and to measure the robustness of a process output under shifting environmental conditions.	Might require a higher number or runs to account also for NFs.
MDs	Allow to analyze complex mixtures with potentially high number of components	Each mixture component covariates with the other, making difficult to estimate the effect of each CPP.

output, and often are difficult to control by the operator, but they can still significantly affect the results. Examples of these variables can be different instruments or operators. It is thus possible to account for these nuisance factors by performing blocking on the experimental runs.

- c. Full factorial design (FFD): This is a combinatorial design in which each of the factors assumes two levels only, and all the possible combinations of factors levels are tested (often indicated as -1 and +1 for the lower and higher values, respectively) (Fig. 8C). In this case, the number of runs can be calculated by the formula  $n = 2^X$ , where n is the number of runs and X the number of factors in study. When it is possible to obtain all the combinations of the factors, the design will result fully orthogonal, with no confounding between the factors. When possible, it is also worth randomizing the design, block it, and add center points (normally indicated using the number 0). Of note, it is possible to create these designs by mixing factors with a variable number of levels, depending on the requirements of the study. However, the combinatorial nature of this design can easily require a large number of runs for a large number of CPPs and if each CPP has more than two values.
- d. Fractional Factorial design (FrFD): this design is created as a fraction of a FFD. It is useful especially when dealing with a high number of factors that would result in a prohibitive number of runs. Normally, the FrFD is created as a half ( $2^{X-1}$ ) or as quarter ( $2^{X-2}$ ) of its original FFD. This design fraction often corresponds to one block of the FFD (Fig. 8D) [7,8]. Importantly, when reducing FFR to FrFD a loss of information occurs, often losing the possibility to estimate for higher interaction effects, and thus FrFDs have a lower resolution than FFDs, and aren't orthogonal. Thus, it is necessary to assume the low effect of factors interactions when choosing this design. Thus, FrFDs are only used for preliminary studies to select the most important CPPs for further analysis.

- e. Packet-Burman designs (PBDs): These designs have the advantage of increasing the number of runs but the formula  $n = 4x$  instead of the FFDs  $n = 2^X$ , lowering the number of runs when many factors are included [9]. Despite being very economic, PBDs can be used only for main effects estimations, since the main effects are confounded with two-factor interactions (and have thus only resolution III).
- f. Central composite designs (CCDs, also called Box-Wilson): These designs are created from a FrFD with one center point. However, in this case the design is augmented by adding additional “star points” positioned in intermediate positions between the extremes of the experimental space (Fig. 8E-G) [10]. The position and distance from the center depend on the specific CCD subtype selected, number of runs and the potential blocking. CCDs are classified in:
  - i. Central Composite circumscribed Designs (CCCDs): in this case, the star points are generated by rotating the extreme points on a hyper-spherical shape, slightly enlarging the experimental space. In this way, each factor has five levels. These designs give very good predictions, and allow for orthogonal blocking (Fig. 8E).
  - ii. Central Composite Face-centered Designs (CCFDs): in these designs, the star points are in an intermediate position between the extremes along the margins of the experimental space (Fig. 8F). These designs provide good predictions but, in some cases, cannot estimate pure quadratic effects. In this instance each CPP has four levels. CCFDs do not allow for orthogonal blocking.
  - iii. Central Composite Inscribed designs (CCIDs): These designs can be used when the boundaries of the space are already at their maximum or minimal possible values, and thus it is not possible to expand the experimental space further. Thus, the star points are defined on the extremes of the experimental space and the vertices of the design are inscribed within them (Fig. 8G). Like in CCCDs, each CPP still requires five levels. However, the predictions of these designs are generally less accurate. Importantly, only CCCDs and CCIDs are rotatable.
- g. Box-Behnken designs (BBDs): This quadratic design is composed of experimental runs that are positioned at intermediate points between the extremes of the experimental space (Fig. 8H) [11]. It is thus possible to imagine a hypersphere encompassing all the points of the design and extending slightly outside of the experimental space. BBDs require less runs than other RMS designs when studying less than four factors. Importantly, the predictions of these designs are significantly less accurate in the space close to the “missing” edges of the experimental space, and allow only limited orthogonal blocking.

Of note, two-level designs with center points can only detect quadratic effects by lack-of-fit analysis, but not estimate them, since it is not possible to model them. To estimate quadratic effects, it is necessary to employ RSM design with at least one center point and three levels. Furthermore, for cubic effects at least four level RSM design are required.

- h. Taguchi arrays. An important subset of factorial design is Taguchi arrays [12]. From a mathematical standpoint, these designs are not different from FFDs and FrFDs. However, the Taguchi method is focused on optimizing the robustness of the process outcome, in most cases the performance of a certain device. This is especially important in the case of product development, since it is not possible to control the conditions a certain product would be used outside of the laboratory. The designs can be adapted to this end by using a regular FFD or FrFD to create the experimental set, using the CPPs that can always be controlled or that are used in for example the production process, and thus cannot be changed after the product reaches its point of use (Fig. 8I). However, another design can be generated “around” each experimental run, considering CPPs that can be encountered during product usage, that being NFs (Fig. 8J). This second “outer” array would thus be orthogonal to the “inner” design. Ultimately, these designs would consider both screening for process

**Table 4**  
Summary of all the discussed studies involving DoE application to polymeric nanovectors as drug delivery systems.

Formulation	Design	Software	Process	CPPs	CQAs	Objective	References
PLGA NPs	CCD 16 runs	Statgraphics Centurion	Solvent displacement	Polymer concentration, drug concentration, and surfactant concentration	Size, PDI, ZP, EE	Improve drug residence and penetration in the eye.	[16]
PLGA NPs	Taguchi orthogonal array for screening (8 runs), followed by BBD (17 runs)	Design Expert®	Modified solvent displacement	PLGA conc Pol188 conc Sonication amplitude	Size, PDI, ZP, EE, drug release	Improve CAP efficacy in CRC	[17]
PLGA NPs	PBD (30 runs, for screening), followed by CCD (30 runs for optimization)	Design expert	Modified solvent evaporation	Polymer amount; surfactant concentration; homogenization speed; homogenization time; ultrasonication time	Size, PDI, EE	Improve cilnidipine oral bioavailability.	[18]
PLGA NPs	CCD 26 runs	Statgraphics Plus 5.1	Solvent displacement	pH and Tween 80 concentration in the aqueous solution and concentrations of PLGA and RLZ	Size, PDI, ZP, EE	Improve the ocular delivery of RLZ	[19]
Poly- $\epsilon$ -caprolactone NPs	Factorial design (12 runs) followed by BBD (17 runs)	Design Expert®	Solvent displacement	Polymer and poloxamer concentration, Sitting speed and phases volumes ratio.	Size, EE	Improve oral bioavailability of CIL	[20]
Poly- $\epsilon$ -caprolactone NPs	14 runs screening PBD followed by 46 runs BBD (RSM) for optimization	Minitab (PBD) Design Expert (BBD)	Modified solvent displacement method	Homogenization time, homogenizer speed, Sonication time, Polymer amount, Surfactant amount	Size, ZP, EE	Improve docetaxel bioavailability and efficacy <i>in vivo</i>	[21]
ZNPs	BBD 17 runs	Design Expert®	Nanoprecipitation	volume of the zein solutions, stirring speed, water volume	Size, EE	Drug delivery of DM1	[22]
PLGA NPs	FFDs (screening, 17 runs) followed by SRD (9 runs)	Statgraphics Centurion	Nanoassemblr (microfluidics induced nanoprecipitation)	TFR FRR PLGA; N—Ac ratio PLGA concentration grinding bead volumes	Size, PDI, ZP, EE	Fine- tune particles size and optimize EE	[24]
Cellulose nanosuspension	3 <sup>3</sup> FFD (27 runs)	Design Expert®	Wet milling	different diameter of zirconium oxide beads different milling speeds	Size PDI ZP	improve the oral bioavailability of CsA	[25]
Chitosan NPs	PBD (17 runs) for screening followed by BBD for optimization	Design Expert	Ionic Gelation	amount of chitosan, amount of sodium STPP, pH of STPP, rate of addition of STPP, homogenization speed, duration of homogenization, amplitude of ultrasonication, and duration of ultrasonication	Size, EE	Improve oral bioavailability of tenofovir	[27]
Chitosan NPs	Screening design (18 runs) followed by 18 runs RSM D-optimal design (17 runs)	Design expert	Ionic gelation	Hyaluronic acid, alginate, dextran, their concentration and the concentration of TMC	Size, PDI	Improve the delivery of antisense DNA to tumor cells <i>in vivo</i>	[28]
Gelatin NPs	BBD (15 runs)	Design Expert®	Desolvation	stirring rate, cross-linker solution volume, cross-linking time	Size	Improve pulmonary delivery of methotrexate	[31]
Gelatin NPs	CCD (15 and 11 runs, for nanoprecipitation and for desolvation, respectively)	Design Expert	Nanoprecipitation and desolvation	Gelatin amount, Surfactant amount, GA concentration	Size, ZP, EE	Improve the release of NSAIDs	[32]

**Table 5**  
Summary of studies applying DoE to lipid NPs-based DDSs.

Formulation	Design	Software	Process	CPPs	CQAs	Objective	References
LNPs	FFDs (2 <sup>2</sup> , 5 runs including a center point)	NA	High shear homogenization	Lipids ratio, surfactant ratio	Size, PDI, ZP	Improve NPs biocompatibility for dermal permeation	[34]
LNPs	BBD 19 runs	Design Expert®	High pressure homogenization	drug concentration, concentration of emulsifier, and homogenization pressure	Drug loading (% DL), %entrapment efficiency (%EE), and particle size	Improve availability of RIF	[35]
LNPs	FD (RSM) 32 runs	Design Expert®	High-speed homogenization followed by ultrasonication	Poloxamer and glyceryl monostearate amount	Size, EE Drug release at 8 h and 24 h	Obtain particles with small size, high EE and slow release	[36]
LNPs in hydrogel	1/16 fractional factorial design for screening followed by full factorial design (CCD, 13 runs) for optimization	Design expert	High shear homogenization	CPPs lipid content, mixture types, surfactant: cosurfactant ratio, Surfactant mixture content, dispersion cooling temperature, and homogenization speed	Size, EE, skin retention, skin permeation	Improve itraconazole penetration and efficacy against dermal fungal infections.	[37]
LNPs	CCD 20 Runs	Design Expert®	Ultrasonication and gradual addition of water to the molten lipid mixture	Lipid concentration Dug concentration Surfactant concentration	Size, EE	Improve DCX toxicity against breast cancer cell lines.	[38]
LNPs	2*3 asymmetrical FFD	NA	Ultrasonication and gradual addition of water to the molten lipid mixture	stabilizer concentration and sonication time	Size, PDI, EE	Improve oral availability of Gliclizide	[39]
LNPs	Resolution IV screening design followed by BBD for optimization (17 runs)	Design expert	Solvent evaporation	Amount of lipids, amount of surfactant, volumetric ratio between phases, stirring speed,	Size, EE	Improve cilnidipine oral bioavailability	[40]
Dried pro-liposomes	CCFD 9 runs	Minitab	Layer deposition	Lipids:drug ratio Amount of solid carrier	Size, EE, Release at 6 h	Improve oral bioavailability of lopinavir	[41]
LNPs	FFD	Design Expert®	Microfluidics continuous flow.	Sonication time pH formulation Dialysis buffer	Size, PDI	Fine tune mRNA LNPs size	[45]
LNPs	MD 16 runs	NA	Microfluidic mixing	Molar ratios of ionizable lipids, cholesterol, PEGylated lipid and DOPE as helper lipid	Size, PDI, ZP, EE Change in size during incubation in amniotic fluids	mRNA delivery to fetal tissues	[48]
LNPs	Definite screening design (18 runs) as first step, followed by Taguchi FFD (18 runs) for optimization	JMP	iLiNP microfluidics device	Percentage of PEG, Percentage of cationic lipid, percentage of neutral lipid, identity, of cationic lipid, identity of neutral lipid, mRNA lipid ratio	Particles size, PDI	Optimize liver specificity and liver mRNA expression, spleen Luc expression, liver specificity.	[49]
LNPs	Mixture design 16 runs Followed by higher resolution 12 runs mixture design	NA	Microfluidics mixing	Ionizable lipids, phospholipids (DOPE), cholesterol and PEGylated lipid ratio	Size, PDI, Transfection efficacy, cytotoxicity	Improve transfection of mRNA in T cells while minimizing cytotoxicity.	[50]
LNPs	FFD 26runs	JMP	Micro encapsulate microfluidic system	Carrier lipid identity, Lipid concentration, Particles concentration	Luc expression	Maximize saRNA transfection efficiency	[52]
LNPs	Definitive screening (26 runs) Followed by BBD (26runs)	JMP	Microfluidics	-TFR, temperature of formulation, total lipid concentration, lipids components proportion, different ionizable lipids and phospholipids, pH of the buffer.  -Type and amount of ionizable lipid, amount of phospholipid, and pH of the buffer	Size, PDI Zeta potential, EE, RNA integrity.  Size, PDI Zeta potential, EE, RNA integrity, cytokines production, protein expression.	Optimize protein expression whilst minimizing cellular activation	[53]

parameters to optimize the product features, but also consider the performance variability for the outcome of each run. In this way, it would be possible to understand the factors effect not only on the final outcome, but also on its robustness. Specifically, the standard deviation of each outcome under different environmental conditions, would be a CQA. This approach is very powerful but still requires a higher number of runs compared to the equivalent FFDs without the NFs. It is still possible to reduce the number of runs required by

performing only FrFD on either the “outer” or the “inner” array. Taguchi arrays created from FrFDs are highly efficient in monitoring the potential presence of factor-noise interactions, but not in explaining factor-factor interactions within the inner array. Thus, it is advisable to use these kinds of designs in early screening, when only many main factors effects are considered, and use the variability of the response under noise conditions as just another response to consider when screening in and out the inner array factors.

**Table 6**  
Summary of the studies applying DoE to biotechnological and biomimetic DDSs.

Formulation	Design	Software	Process	CPPs	CQAs	Objective	References
VLPs	BBD 15 runs	R Studio	Sf9 cells infection system	CCI, MOI, TOH	Baculovirus infection, VLP production, VLP assembly, cell viability and VLP productivity	Optimization of VLPs production	[54]
			High five cells infection system				[55]
RBCs membranes-coated LNPs	Full factorial design (25 runs), 3 <sup>2</sup> factorial design (9runs), 2 <sup>2</sup> factorial design, Taguchi array	JMP	-Ultrasonication	-lipid composition, type of surfactant	-Size, PDI, Zeta potential	Improve the delivery of lovastatin and curcumin across the BBB	[57]
			-High pressure homogenization	-Tween concentration, composition of the lipid phase	-Size, PDI, Zeta potential, EE		
			-Co-extrusion with RBCs membranes	-Amount of Tween, production method	-Size and zeta potential		
				-Vol of RBCs, volume of extrusion, concentration of stearylamine	-NPs size and zeta potential.		
Leukosomes	BBD (18 runs)	Statgraphics Centurion	NanoAssemblr	TFR FRR Lipid:proteins ratio	Size, PDI, Zeta potential	Improve the targeting of inflamed endothelial cells and cytotoxic effect in tumor cells.	[58]

**Table 7**  
Summary of studies applying DoE to hybrid DDSs.

Formulation	Design	Software	Process	CPPs	CQAs	Objective	References
Lipidoid-PLGA particles	3 <sup>2</sup> FFD (17 runs)	Design Expert®	Double emulsion	Lipidoid content and lipidoid:siRNA ratio	Size, PDI, ZP, EE, toxicity, transfection efficacy	Improve the pulmonary delivery of siRNA	[63]
Lipidoid-PLGA particles	3 <sup>2</sup> FFD (17 runs)	Design Expert®	Freeze drying	lipidoid content and lipidoid:siRNA ratio	Size, PDI, ZP, EE Transfection efficacy, toxicity	siRNA delivery to lung cancer	[64]
Lipidoid-PLGA particles	I-optimal RSM custom design (25 runs including replicates)	Design Expert®	Double emulsion and freeze drying to create the dry formulation	lipidoid content and lipidoid:siRNA ratio	Size, PDI, ZP, EE Transfection efficacy, toxicity	Improve anti TNF- $\alpha$ delivery to the lungs	[65]
Lipidoid-PLGA NPs	One factor-at a time	NA	Double emulsion	amount of ionizable lipid (L5) and the L5 to ASO ratio	Size, PDI, ZP, EE High transfection	Improve ASO delivery	[66]
LPHNPs	FFD (8 runs)	Design Expert®	Single-step nanoprecipitation	PLGA amount, lecithin/PLGA ratio (w/w), and Tween 80 concentration	Size, PDI, EE	Improve delivery of RU across the BBB	[67]
Lactoferrin-functionalized-TMC-PLGA NPs	BBD (17 runs)	Design Expert®	Solvent displacement	Polymer, drug, and surfactant amount	Size, EE	Improve the nasal delivery of Huperzine A	[69]
Lipid-polymer crystalline NPs	FD (2 <sup>3</sup> , 11 runs including three center points)	Design Expert®	Micro-emulsification followed by sonication	Amount of docetaxel, amount of Pluronic F68 and F127.	Size, PDI, ZP	Improve docetaxel delivery	[70]
PDLG-gelatin NPs	3 <sup>3</sup> FFD (27 runs)	Design Expert®	Emulsification	percentage of internal phase, percentage of gelatin and percentage of PDLG	Size, PDI, MDT, K, T25%	Improve piroxicam pharmacokinetics after intra-articular injections.	[71]

i. Mixture designs (MDs). MDs are arrays in which each CPP considered is a component of a mixture and overall sum of the different component proportions will always be 100%. When imagining the geometry of a MD, it is possible to obtain the space by connecting non-adjacent points in an FFD array, in which the boundaries are the diagonal across each face of the array (Fig. 8K). This shape is defined as a simplex, and can be represented as a triangle for three components. Thus, when changing a single component, all the other factors also change proportionally. This makes the factors co-variant, and therefore the assessment of a single component statistical significance is confounded by the others. The two main types of MDs are:

- Simplex lattice: in this design, all the experimental points are on the boundaries of the simplex, and are equidistant from each other

(Fig. 8L). This design includes thus pure mixtures with only one component at vertices of the simplex, and different proportions of binary mixtures, depending on how many levels for each component are selected. In this way, the experimental points are evenly dispersed across the simplex axes.

- Simplex centroid: It is possible to augment the design by adding central point in the middle, obtaining a centroid design which allows to understand the mixture behavior within the center of the simplex space (Fig. 8M).

Simplex designs can be enhanced by adding check points in between the center and the vertices. These points have similar functions to center points in regular factorial designs, allowing for the estimation of potential curvature in screening objectives, and potentially modeling more complex models when applying RSM.

**Table 8**  
Summary of studies applying DoE to different colloidal DDSs used to improve drug solubility.

Formulation	Design	Software	Process	CPPs	CQAs	Objective	References
Carvedilol co-crystals	CCD 30 runs	Design Expert®	Solvent displacement with sonication	concentration of CAR, of conformer, of poloxamer 188, and AS/S	Size, PDI, ZP	Improve carvedilol solubility and bioavailability	[72]
Nanosuspension	CCF 20 runs	Design Expert®	Nanoprecipitation	Concentration of EM, concentration of the stabilizer (soluplus) and ultrasonication intensity	Size, PDI	improve the solubility and bioavailability of EM	[73]
Peptide-DNA NPs	FFD 19 runs	Design Expert®	Spray drying	mannitol concentration, inlet temperature, spray rate, and spray frequency	process yield, DNA recovery, moisture content, Size, zeta potential, EE	Achieve pulmonary DNA delivery	[74]
Hesperidin nanocrystals	Screening design (11 runs) followed by a RSM design (11 runs)	MODDE	Spray drying	Inlet temperature, amount of protectant and feeding rate	Size	Minimize nanocrystals size, thus improving hesperidin solubility	[76]
Lam-PVA NPs	FFD (30 runs, 3 center points)	MODDE	Dry milling	Milling time, milling speed, PVA:Lam ratio	SIZE, PDI, release after 5 and 10 min	Improve the nasal bioavailability of LAM	[77]
Clotrimazole-cellulose dry nanosuspension SNEDDS	BBD 15	Minitab	Hot melt extrusion	Feed speed, inlet temperature, Screw speed	PDI Moisture content	Increase drug solubility and release	[78]
SNEDDS	MD 16 runs	Design Expert®	Emulsification by addition of water to the oil-drug-surfactant mixture	the oil (palm oil), the surfactant (Capmul® MCM), and co-surfactant (Tween 80).	Size, turbidity	increase the oral bioavailability of PTX	[80]
SNEDDS	MD (7 runs followed by smaller design)	NA	Emulsification by addition of water to the oil-drug-surfactant mixture	Oil, cosolvent and surfactant	Size, Transmittance, emulsification grade, EE	Improve the solubility and release of celecoxib and fenofibrate (model drugs)	[81]
MTB lyophilized nanovaccines	Custom designs from JMP software (40 runs, 12 runs, and 15 runs respectively)	JMP Pro	Antigen dissolution in excipients and lyophilization	DoE1: disaccharide type (trehalose or sucrose) and concentration (3.5%–10%, w/v), mannitol concentration (0–1%, w/v), buffer type (20 mM Tris or sodium phosphate), and pH  DoE 2. glycine and mannitol concentration  DoE3: actors were disaccharide type (trehalose or sucrose) and concentration (2.5%–10%, w/v)	Size change after reconstitution, cake quality after lyophilization, stability and immunogenicity <i>in vivo</i>	Improve long term vaccine stability while retaining immunogenic activity	[82]

Importantly, different designs can be assembled with each other, depending on the nature of the different factors considered (qualitative, quantitative, or mixture). For example, a MD can be combined with an FFD. One way to visualize their structure would be to imagine that each experimental point of a factorial design actually corresponds to a mixture simplex (or *vice versa*). Nowadays, the operator can just specify the number, levels and type of CPPs, select a specific objective, resolution level, number of center points, blocking and randomization in the software and the software can either suggest a type of design or generate a brand-new design different from the classical arrays summarized in this section.

## 6. Analysis workflow for DoE

1. The first step is inspecting all the data for outliers and possible typos by creating several graphs to get the wider picture of the data. These include graphs with data plotted across time, across blocks, and across the experimental space. It is also important to check for the variability of the results, and in particular their normal distribution.
2. The next step is the creation of the model. Model selection and methods of data interpolation are limited by the experimental design itself, since the number and position of experimental runs in the design array and the design proprieties themselves are based on the

operator decisions at the moment of design selection. Importantly, the model can be improved manually by performing a stepwise regression, and it is work performing a trial-and-error process to find the best model fit. It is possible to apply an additive strategy, adding one CPP at the time until optimal interpolation is reached, or a subtractive strategy can be used, removing progressively non-significant factors to improve the model fit. It is important to pay a lot of attention to this step, because the final model will define which CPPs will be used for future experiments and for potential RSM predictions. It is also important to test the model assumptions. This can be performed with residual graphs. If the model is not violated, it is possible to proceed, otherwise, it could be necessary to adjust the model or transform the data (e.g. put data as logarithms, percentages, normalize them when possible).

3. Then the model can be used to assess the CPPs significance and perform RSM optimization. This is often performed using desirability functions.
4. If the design was used for optimization, validate the model predictions with multiple runs of the optimized settings.

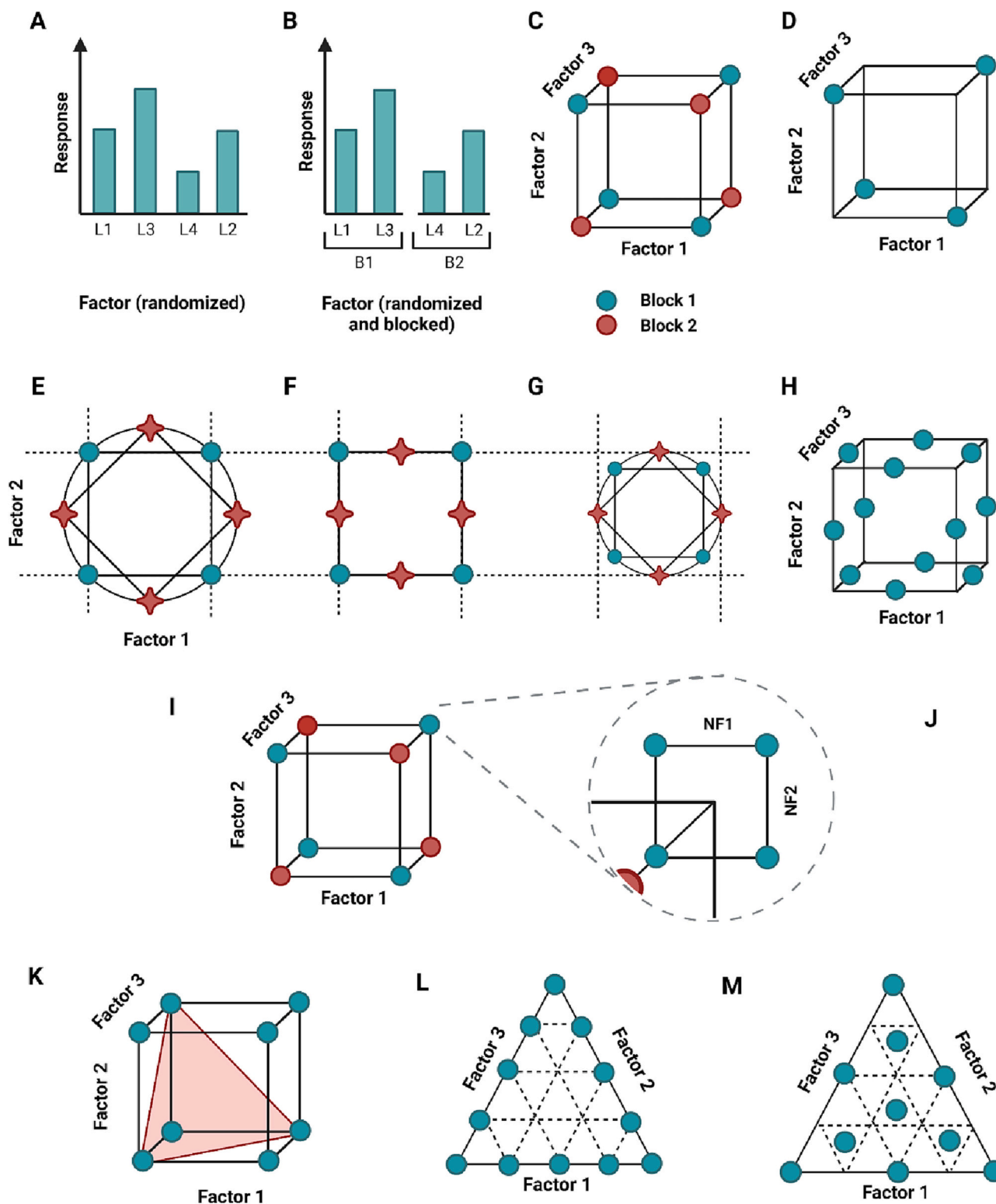


**Fig. 8.** Schematic representation of a single factor randomized (A) and blocked (B) design, a three-factors FFD blocked (C), a FrFD (D), a two factors CCFD (E), a CCFD (F), a CCID (G) and a BBD (H). Representation of an FFD (I) which includes NFs according to a Taguchi array (J). Three factors geometrical representation of a MD construction (K, red surface). Representation of a Simplex lattice design (L) and a Simplex centroid design (M). This figure was generated using [Biorender.com](https://www.biorender.com). (For interpretation of the references to colour in this figure legend, the reader is referred to the web version of this article.)

## 7. Current DoE applications in nanomedicine

### 7.1. Synthetic and natural polymeric nanovectors

Polymeric DDSs have been widely applied in many pathological

settings to improve the pharmacokinetics of small molecules and biotechnological therapeutics [13,14]. The most used formulation process for these DDSs is the solvent displacement method, in which the drug and polymer are solubilized in an organic solvent which is then gradually added to an aqueous phase, with the polymer precipitation

and consequent nanoparticles (NPs) self-assembly caused by solvent evaporation or by dispersion of a miscible organic solvent in the aqueous phase. The size of polymers droplet is normally reduced by homogenization mechanic stirring, sonication, or a combination thereof.

This approach has been applied to the production of NPs using the biodegradable, FDA-approved poly-lactic-co-glycolic acid (PLGA) [15] and poloxamer 188 (P188) to deliver fluorometholone (FMT) for the treatment of eye inflammation [16]. The optimized formulations (7.0 mg·mL<sup>-1</sup> of PLGA, 15 mg·mL<sup>-1</sup> of P188 and 1.5 mg·mL<sup>-1</sup> of FMT) showing a slower release and improved eye permeation than an FMP commercial formulation (Isoptoflucon®) as well as showing improved efficacy compared to Isoptoflucon® in an *in vivo* swine model of ocular inflammation. Another analogous study implemented this approach to encapsulate the ant colorectal cancer drug capecitabine (CAP), obtaining NPs with slow release *in vitro*, improved cytotoxicity in HT-29 CRC cells compared to free CAP [17], and ultimately higher bioavailability in mouse models. All these studies, despite applying different designs demonstrated how NPs size and EE is increased by increase in the amount of polymer and drug in the organic phase, since in this case there is more bulk material to constitute the particles. On the other hand, more surfactant concentration decreased NPs size thanks to its ability to reduce the surface tension among phases, diminishing also the PDI, but also decreased EE, since the smaller particles have higher interfacial surface that favors drug leakage. When applied, homogenization speed or sonication time or amplitude decreased NPs size due to higher mechanical stress reducing the particle size.

Another similar application of PLGA particles was the delivery of the antihypertensive drug cilnidipine (CIL) [18], with optimal formulations demonstrating long colloidal stability and drug retention, slow drug release, amorphous structure, and greatly improved drug bioavailability *in vivo* compared to free drug in murine models. In this case however, surfactant concentration increased the NPs size, perhaps due to higher interactions among its molecules causing the fusion of organic phase droplets. This underlines how each material can have different effects on a similar process, depending on its properties.

Notably, another investigated variable was pH of the aqueous phase. Specifically, a recent work by Esteruelas et al. [19] demonstrated how higher pH decreased the size and PDI, ZP and EE of PLGA NPs loaded with the anti-glaucoma drug riluzole (RLZ). Interestingly, in this case the Tween 80 used as surfactant increased EE. The causes of pH influence on particles features is not clear since the polymer and surfactant are both non ionizable. The optimized formulation in this case resulted in a Tween 80 concentration of 3.5% (w/v), a RLZ concentration of 1.5 mg/mL, a PLGA concentration of 8 mg/mL, and a pH of 5. With particles size below 200 nm, negative ZP, PDI below 0.2, and EE above 90%.

Solvent displacement was also applied by Diwan et al [20] optimized the formulation of poly-ε-caprolactone NPs prepared by nanoprecipitation to improve the oral bioavailability of CIL, confirming the positive effect of polymer amount on size and EE. Similar results with this polymer were also observed by Vardhan et al. [21], who focused on poly-ε-caprolactone NPs optimization to improve the pharmacokinetics and efficacy of the antitumor drug docetaxel (DTX) using a modified emulsification and solvent displacement approach. This study also confirmed the negative effect of sonication time and homogenization on NPs diameter.

Another work by Yu et al. [22] focused on the optimization of zein nanoparticles (ZNPs) as drug delivery platform for the antitumor drug maytansine (DM1). ZNPs were prepared by precipitation of a zein and DM1 DMSO solution in water. The authors applied a BBD to assess the effects of the volume of the zein solutions, stirring speed, water volume on final drug encapsulation. Despite not offering much information on the statistical relevance of the single factors and their interaction into the process, this design allowed to obtain ZNPs with suitable size and high encapsulation efficiency. These particles demonstrated high uptake and improved cytotoxicity against A549 lung cancer cell lines. Ultimately, DM-1 loaded ZNPs demonstrated improved accumulation and

antitumor efficacy in subcutaneous models of lung cancer.

An alternative approach to solvent displacement are microfluidics. These approaches result more controllable and scalable than traditional solvent displacement. The most widely applied microfluidics system used for DDSs formulation is the Nanoassemblr™ device. This instrument allows quick and reliable NPs production through the fast microfluidic mixing of an organic phase containing lipids or polymers, and a miscible phase that is miscible to the former. Their blending causes a change in polarity in the mixture and induces the self-assembly of NPs by precipitation [23].

Chiesa et al. [24] focused on the optimization of PLGA particles using NanoAssemblr™ employing as model drug *N*-acetylcysteine (N—Ac). The selected CPPs were the flow rate ratio between the two phases in the device (FRR aqueous: organic), the total flow rate in the system (TFR), the PLGA concentration, and polymer:drug ratio. The NPs size was negatively influenced by the TFR and FRR due to higher shear stress that reduces NPs size and lower polymer concentration during the mixing, respectively. Of note, EE was influenced by the TFR and FFR positively but negatively by their interaction, while higher drug: polymer ratio also increased it. This significance was confirmed by a subsequent RSM 3<sup>3</sup> design, obtaining an optimal formulation using 13 mL/min TFR and a 1:4 FRR. Another RSM extrapolation was performed and obtaining a similar optimized formulation with high EE (TFR = 15 mL/min and FRR = 1:5).

More traditional formulation processes have also been used in conjunction with DoE. One such instance is offered by Pinar et al [25] who focused on the optimization of a wet milling process to produce a cellulose nanosuspension to improve the oral bioavailability of the immune-suppressive drug Cyclosporine-A (CsA). The CPPs employed in this study were grinding bead volumes, the different diameter of the beads, and the different milling speeds; and the CQA were particles size, PDI, and ZP. The study was performed using a three level 3<sup>3</sup> FFD. Bead diameter and milling speed were identified as the most important factors. In particular, smaller bead diameter, higher beads volume and higher speed led to smaller particles due to higher shear stress applied on a larger surface of the NPs mixture. Smaller beads and lower speed also decreased the PDI. The optimal formulation was thus produced using high milling speed (600 rpm), low bead size (0.1 mm), and high bead volume (25 mL), and resulted in particles with 561.2 nm size, 0.374 PDI, and - 24.4 ZP. The particles were colloiddally stable over 9 months, improved CsA apparent solubility, showed slow drug release in acidic pH, but fast release in simulated intestinal fluids, and improved CsA bioavailability in fed rat model, albeit slightly lower in fasting animals compared to the current CsA commercial product (Sandimmun Neoral®).

Ionic gelation allows the formulation of gel NPs by gradually adding a negative ion to a positively charged polymer and drug mixture, inducing its gelation under stirring in gel NPs [26]. Shailender et al. [27] performed the optimization of chitosan NPs to improve the enteric bioavailability of the antiretroviral prodrug tenofovir disoproxil fumarate using ionic gelation. The authors applied a low resolution PBD to screen out some CPPs among the ones selected: amount of chitosan, amount of sodium tripolyphosphate (STPP) used as gelation agent, pH of the STPP solution, rate of addition of STPP, homogenization speed, duration of homogenization, amplitude of ultrasonication, and duration of ultrasonication. The CQAs were NPs size and EE. The only three CPPs selected for the further BBD-based optimization were chitosan amount, amount of STPP and duration of sonication. As shown in above mentioned studies, NPs size was increased by chitosan amount and by STPP, but decreased by sonication time, with a similar trend also for EE. The optimized formulations demonstrated a suitable size of 200 nm, PDI around 0.2, slightly negative ZP, and 50% EE. The particles demonstrated improved intestinal permeation using *ex vivo* inverted rat intestinal sacks. Furthermore, oral administration *in vivo* in rats demonstrated superior bioavailability compared to the free drug.

Similarly, Baghaei et al. [28] optimized polymeric NPs using either

alginate, hyaluronic acid, or dextran as gelation agent to prepare trimethylchitosan (TMC) NPs to deliver DNA encoding for an antisense sequence of the Human SET1 (h-SET1). This oligonucleotide exerts antitumor activity by interfering with histone methylation [29]. The authors selected as CPPs the polymer concentration and the concentration of gelation agents. They demonstrated that particles size and PDI decreased with lower polymer concentration. Furthermore, the authors performed a second D-optimal design for NPs optimization using only different polymers and polyelectrolyte concentration as CPPs. Hyaluronic acid showed the best features as gelation agent with a concentration between 0.2 and 0.47 mg/mL of TMC and hyaluronate: 0.35 mg/mL. Indeed, the particles demonstrated a size around 50 nm, low PDI and almost 100% DNA EE. The NP also reached the tumor mass after intravenous injection in 4 T1 xenograft mouse model.

Another polymeric NPs formulation process is the induction of proteins and drugs precipitation by changing the polarity of their solution using an organic solvent and inducing the assembly of particles using a chemical crosslinker, in a process defined as desolvation [30]. This approach was used Abdelrady et al. [31] for the optimization of gelatin nanoparticles for the pulmonary delivery of methotrexate (MTX) against pulmonary cancer. This work employed gelatin as polymer, acetone as desolvation agent, and glutaraldehyde (GA) as crosslinker. A BBD with three levels was employed, considering the stirring rate, cross-linker solution volume, cross-linking time. The aim of the design was to optimize particles size to improve their pulmonary delivery by inhalation. The study demonstrated that it was possible to reduce the particles size, as well as increasing the stirring speed during the process. The process yielded gelatin NPs formulation with suitable features and in accordance with the predictions, slow trypsin-dependent MTX release, good *in vitro* uptake by macrophages and lung cells, improved cytotoxicity compared to free MTX, and importantly, suitable aerodynamic proprieties for lungs deposition after inhalation.

Koletti et al. [32] focused on the optimization of gelatin NPs to improve the administration of non-steroidal anti-inflammatory drugs (NSAIDs) prepared by desolvation and nanoprecipitation. For both formulative approaches, the authors employed a first one-variable-at-a-time approach to find the best desolvation agent and surfactant type for the nanoprecipitation, demonstrating that particles size increased using polysorbate 20 and 80 instead of poloxamer 408 and 188. Furthermore, ethanol as desolvant led to smaller NPs. Thus, the authors employed poloxamer 407 as stabilizer and acetone as desolvant. Then the authors applied a CCD to screen the effect of stabilizer's concentration, gelatin's content, and glutaraldehyde content on the NPs size and zeta potential. All three factors had influence on the CQAs: gelatin content increased particle size, as did to a lesser extent GA concentration. The ZP acquired more negative values at intermediate values of gelatin concentration and at either the highest or lowest poloxamer concentration. Gelatin content also increased EE. Furthermore, increasing glutaraldehyde decreased ZP to more negative range. The same process was applied to desolvation using acetone, gelatin type B and gelatin stiffness as CPPs, applying a CCD. In this case, size was higher at highest and lowest amounts of gelatin, and smaller at the extremes of GA concentration range. ZP in this case became more negative with increasing the amount of gelatin. Gelatin content also increased EE. Of note, to create predictive models for optimization, the authors used in parallel a traditional multiple regression analysis approach, and also applied artificial neural networks (AI) with the aim to improve the accuracy of the models. Despite the neural networks performing a better statistical interpolation of data thanks to their higher computational power, the predictions were quite similar between the two modeling strategies. The optimized formulations showed a desirable small size, high EE, slow two phasic drug release.

## 7.2. Lipid NPs

Lipid NPs (LNPs) have been widely applied to improve the delivery

of poorly soluble drugs [33]. High shear homogenization and emulsification allow to efficiently mix lipid and drug mixtures with a hydrophilic phase, forming small NPs. This process is not dissimilar from solvent displacement, although in this case the organic solvent is substituted by a molten lipids' solution. This process was applied in a study from Rigon et al. [34] to improve LNPs for the dermal delivery of pharmaceuticals through improved permeation. The CPPs considered were the ratios of the LNPs components (stearic acid: behenic alcohol ratio) and the ratio of surfactant (poloxamer P40) compared to total lipids. As usual, the CQAs selected by authors were the size, PDI, and ZP. The only statically significant CPPs were the positive influence of lipids ratio and poloxamer ratio in particles size, with PDI and ZP not being affected by these factors. The formulation that was optimized from this screening resulted have suitable size, homogenous distribution, and biocompatible ZP, with only toxic effects only at high doses on mouse fibroblasts.

Chokshi et al. also [35] optimized LNP using high pressure homogenization to improve the bioavailability of the antituberculous drug rifampicin (RIF). In this study, the authors employed an RSM through a three-level, three-factor Box–Behnken design. The considered CPPs were drug concentration, concentration of emulsifier, and homogenization pressure. Increasing the surfactant (poloxamer 80) concentration reduced significantly particles size and EE. Of note, the number of homogenization cycles decreased particles size and PDI due to higher shear force, as did the homogenization pressure. At the same time, increasing the drug concentration also increased the EE and DL, and only slightly size and PDI, similarly to the trends observed in solvent displacement. After performing data interpolation, the optimized formulation required the following settings: concentration of RIF = 30% w/w, concentration of S80 = 0.1963% w/v, and homogenization pressure = 952.2 bar. This formulation when prepared demonstrated a size of 445.2 nm, %EE of 84.24%, and %DL of 15.79%, in good accordance with the predicted values. Ultimately, these particles demonstrated a spherical, solid amorphous structure, with a slow RIF release profile.

Similar trends in CPP influence were also observed by Pandey et al. [36] performed the optimization of a solid lipid NPs formulation to improve the efficacy if the antidiabetic drug glibenclamide, as did Kumar et al. [37] who focused on the optimization of LNPs to improve the topical delivery if the antifungal drug itraconazole. The authors selected as CPPs to be screened lipid content; mixture types; surfactant: cosurfactant ratio; Surfactant mixture content ( $S_{mix}$ ); dispersion cooling temperature; and homogenization speed, and as CQAs the particles Size, skin retention and skin permeation, performed on rat skin *ex vivo*, and EE. After selecting as only relevant CPPs the lipid content and  $S_{mix}$ , the authors performed a second FFD to optimize NPs composition. Both CPPs increased EE; particle size increased mainly with the lipid content, as expected, and skin retention increased also with both CPPs, perhaps because of overall higher drug encapsulation. However, skin permeation was optimal only at intermediate lipids and  $S_{mix}$  amounts, since only a certain amount of lipids and surfactants can improve skin permeation and hydration without interfering with drug release itself. The authors thus validated the optimized formulation by producing LNPs with 4.58% (w/v) of Compritol C888 and 2.94% (w/v) of  $S_{mix}$  content. The LNPs demonstrated a size around 260 nm with positive ZP, high EE, with skin retention and permeation superior to the current commercially available creams with same application. Furthermore, the optimized formulation demonstrated good skin tolerability and improved efficacy, removing dermal fungal infection on rats 25% faster than the commercially available formulations.

Rarokar et al. [38] obtained analogous results by employing DoE to improve the formulation of LNPs for docetaxel (DCX) delivery against breast cancer cells. The model was then validated by formulating an optimized particle batch, which demonstrated suitable features (size around 200 nm and EE above 90%), slow drug release, and improved cytotoxicity compared to the free drug in MDA-MB-231 triple negative breast cancer cells.

Nazief et al. [39] confirmed these trends when studying LNPs to deliver orally the anti-diabetes drug gliclazide with improved bioavailability. The authors used a 2<sup>3</sup> asymmetrical factorial design to study the effect of stabilizer concentration and sonication time on the particles size, PDI, and EE. Despite this study using ultrasonication and not homogenization to disrupt the lipid phase, increasing the surfactant concentration still decreased particles size. Notably, both time of sonication and stabilizer concentration showed minimal PDI at intermediate values. EE had a complex function, since it was negatively affected by increase in surfactant at short sonication time, but presented a bell profile at thigh sonication times. Ultimately, the optimized formulation resulted to be 150 mg poloxamer, 10 min sonication, presenting suitable 245.9 nm size, and a PDI of  $0.482 \pm 0.026$ , with high EE. These particles demonstrated a spherical shape, a slow drug release, and improved the drug bioavailability compared to free gliclazide, with no visible sign of gastrointestinal or systemic toxicity in rats.

LNPs can also be produced similarly to polymeric NPs using a solvent displacement approach, as did Diwan et al. This time the authors focused on the encapsulation of CIL in LNPs Compritol 888 ATO and poloxamer 188 [40]. A resolution IV screening design was applied, including as CPPs the lipid, concentration of surfactant, ratio of internal to external phase volume, magnetic stirrer speed and temperature effect on particles size and EE. Out of this screening, the authors selected only the relevant CPPs: lipid amount, the ratio of internal to external phase volume, and temperature to perform a BBD. This latter design evidenced how the lipid amount had a positive effect on NPs size, while the phase ratio and the temperature had negative effect perhaps due to lower viscosity of the internal phase caused by dilution of lipids in a higher organic solvent volume. Differently from before, lipid amount had a negative effect on drug loading, perhaps due to internal phase oversaturation, and the phase ratio had only a small positive effect. The resulting optimized formulation had a size around 100 nm with a PDI below 0.25, was stable for over 3 weeks under storage, and presented a slow drug release. Furthermore, the optimal formulation increased by a lot the CIL oral bioavailability in mice, resulting also in bigger decrease in blood pressure over a longer time compared to the free drug.

Patel et al. [41] focused on the optimization of a solid proliposomes powder encapsulating the antiviral drug lopinavir to increase its oral bioavailability, using a layer deposition approach. After performing CQAs risk assessment, the study focused on a 9 runs FCCD to optimize the lipids:drug ratio and amount of polyalcohol carrier used in the layer disposition approach used for formulation. As expected, EE increased with an increase in lipid:drug ratio, while NPs size decreased in the higher range, and drug release had a curved response with higher release in the intermediate range of lipid:drug ratio. On the other hand, the amount of medium mainly decreased the NPs size. The generation of the model and the application of constraints on liposomes features (vesicle size <500 nm, %EE > 85% and drug release >90% in the first hour) allowed to define a small experimental space in which the formulation would be more robust. The optimized particles after reconstitution demonstrated a size of 660 nm, an EE around 90%, a PDI around 0.1, and a negative ZP, all suitable features to increase lopinavir delivery. The NPs demonstrated an amorphous state and improved lopinavir permeation across Wistar rats' intestinal sections *ex vivo*, and even more than double C<sub>max</sub> and bioavailability after *in vivo* oral administration.

LNPs have also been widely used as DDSs for the administration of polynucleotides, including DNA [42], siRNA [43], and mRNA [44]. This explosion of application was sparked by the invention of cationic and then ionizable lipids which are able to complex and encapsulate polynucleotides and allow them to cross the cellular barrier.

Nag et al. [45] employed DoE to establish a novel and highly scalable flow process for the preparation of LNPs to deliver mRNA. This system offered the possibility to modulate the flow conditions, the buffer pH during formulation, the time of low intensity sonication after mixing, and the final buffer of dialysis, to fine-tune the LNPs size. Obtaining particles with precisely defined sizes would allow to modulate particles

behavior and targeting [46]. In this case, the authors applied a factorial design with five levels of sonication times, three levels of pH, and three replicates (blocks), divided among three buffer groups, to a total of 54 formulations. Notably, sonication time (0 to 100 s) and pH levels (4.2 to 5) were proportional to particles size, obtaining particles in a range of 50 to 200 nm. Furthermore, PDI was higher when sonication time was low and pH low or both CPPs were high. The different buffers used for dialysis (PBS pH 7.4, PBS pH 7.2, HEPES pH 6.7, and HEPES acetate pH 6.7), also influenced the size (with bigger particles for PBS 7.4 and HEPES pH 6.7), while the buffer concentration was not too relevant on the final particles' diameter. On the other hand, buffer concentration (75% to 90%) influenced in a "U" shape the NPs PDI, with lowest values at intermediate percentages. These models were validated across all the experimental space with seven formulations. All these formulations could be easily scaled-up to very high volumes. Finally, the obtained LNPs loaded with COVID-19 spike protein mRNA elicited good antibody response *in vivo* after intramuscular administration in rabbits. As previously reported in the literature, particles with size above 120 nm did not show much antibody response [47]. This system represents a novel and powerful tool to produce new LNPs mRNA formulations.

Swingle et al. [48] instead focused on the optimization of LNPs prepared using a microfluidics device for the delivery of mRNA to fetuses within the amniotic fluid. The authors focused on a MD of 16 formulations with different molar ratios of LNPs components (ionizable lipids, cholesterol, PEGylated lipid and DOPE as helper lipid). The most notable trend in this design was a decrease in ZP with an increased amount of PEGylated lipid. Out of the 16 formulations, seven were screened out since did not have suitable features, including too large size or too high PDI. Two formulations (A5 and A12) with the smaller size and PDI, and highest encapsulation efficiency and were used for further studies. Interestingly, when performing stability studies in mouse amniotic fluid, the A5 particles increased substantially their size and PDI, while A12 formulations became slightly bigger because of the protein corona formation, but resulted stable, as indicated by the PDI. A12 showed also the highest luciferase (Luc) mRNA transfection efficiency in HeLa cells with and without the presence of mouse amniotic fluid. Notably, Luc expression was increased by higher amount of cholesterol in the molar ratio of the particles, and by lower PEGylated lipid percentage, because of improved membrane disruption capabilities, and lower steric hinderance to cellular adhesion, respectively. Notably, A12 particles also showed improved transfection efficacy of luciferase (Luc) mRNA *in vivo* after intra-amniotic injection in pregnant mice compared to A5 particles, reaching fetal tissue and accumulating principally into the fetuses' liver.

In a similar work, Hashiba et al. [49] studied LNPs to deliver mRNA to the liver formulated with a microfluidic device and Luc mRNA as model cargo. Of note, this study applied *in vivo* models from the very beginning of the screening to investigate LNPs transfection efficiency, including as responses not only Luc signal but also liver specificity, expressed as liver Luc signal over overall body Luc signal. To this end, the authors performed a screening design to select only relevant CPPs. From this first screening, the cationic lipid identity and percentage, the PEG percentage, and the neutral lipid percentages were selected for further optimization. For the second optimization DoE, the authors employed a Taguchi FFD, selecting as cationic lipid CL4H6, increasing the range of cationic lipid percentage, and lowering the neutral lipid percentage range, ultimately working in a smaller experimental space. The second screening revealed how CL4H6 and PEGylated lipid proportions increased LNPs size, while neutral lipid and PEG percentage were the most relevant CPPs in increasing liver expression of Luc. According to the second design, the LNPs with composition CL4H6/ESM/Chol/PEG-DMG at a molar ratio of 60/5/35/1.5 demonstrated optimal Luc expression and specificity. Indeed, these optimized LNPs demonstrated high erythropoietin expression in mice and high liver accumulation. Notably, this study also investigated possible correlations between different responses, such as a positive correlation between

LNPs size and liver expression, demonstrating the possibility to apply multivariate analysis on top of DoE to elucidate complex interplays between NPs features and their biological behavior.

LNPs can also be used as transfection agents to enable advanced cell therapies. An example of this strategy is offered by Billingsley et al. [50] who employed LNPs to transfect mRNA for the production of CAR-T cells with minimal cellular toxicity. The authors implemented a first 16 runs screening design testing different proportions of the different lipid components of LNPs and comparing them to a state of the art LNPs formulation. The authors evidenced how formulations with higher ionizable lipid ratios showed improved delivery with higher phospholipid concentrations ratios and at the same time with lower cholesterol in the mixture. Similarly, formulations with higher DOPE ratios benefitted from more ionizable lipid and less cholesterol. These trends suggested that LNPs with increased ionizable lipid and phospholipid ratios and with reduced cholesterol improved mRNA delivery to Jurkat cells. These findings were used to generate a more restricted 12 runs design with a smaller range of components ratios but higher resolution. The optimized formulation resulting from this optimization process demonstrated a 3-fold increased transfection efficiency compared to previous LNPs with minimal cytotoxicity. This formulation was further validated in primary T-cells demonstrating comparable transfection efficacy but significantly reduced cytotoxicity in comparison with electroporation. This in turn translated to comparable tumor killing of acute lymphoblastic leukemia cells by the CAR-T cells. This study has the important feature of validating its findings in patient-derived human T-cells, which highly increases its translational potential. However, the authors do not provide much information on the properties of the employed design, somewhat limiting our understanding of the study itself.

Self-amplifying mRNA (saRNA) consist in mRNA construct that contain sequences encoding for a viral mRNA-dependent RNA polymerase, which allow its self-amplification after transfection, potentially boosting protein expression [51]. Blakney et al. used LNPs to deliver saRNA to the human skin [52]. The authors applied an FFD to produce particles using a microfluidic system and considering as CPP complexing lipid identity (C12–200, the zwitterionic lipid cephalin, DDA, DOTAP), lipid concentration, NPs concentration, and ratio of cationic lipid to cephalin. The authors used as main endpoint the expression of *ad hoc* engineered saRNA expressing firefly Luc, used as model payloads in clinical human skin explants. The authors demonstrated how cephalin was the complexing lipid with highest efficiency, while DOTAP decreased significantly the Luc expression. Furthermore, high lipids and high LNPs concentrations demonstrated increased mRNA expression. Using a similar enhanced green fluorescence protein (eGFP) saRNA construct, the authors also analyzed which were the cells subpopulations responsible for LNPs uptake. Unsurprisingly, although most of the skin explants are constituted of epithelial cells, a disproportionately big fraction of the signal was expressed by the minority of immune cells naturally present in the skin (*i.e.*, dendritic cells, T-cells, monocytes, and Langerhans cells), and the expressions levels were 6-fold higher compared to the standard formulation used as comparison.

Ly et al [53] also employed LNPs to deliver saRNA comparing it to mRNA. The authors employed a two-steps iterative approach to optimization, using first a definitive screening design to screen the main effects of CPPs such as the lipids proportions, the total lipid concentration, the temperature of formulation, the N/P ratio between ionizable lipid and nucleotides, the type of cargo (mRNA versus saRNA), different types of phospholipids and ionizable lipids, different TFRs used during the LNPs microfluidics fabrication, and pH of the aqueous buffer used during synthesis, while the CQAs were particles size, PDI, ZP, EE, and RNA integrity. The first screening revealed that all factors affected to some extent on the CQAs in the study. However, to proceed with the second step, the authors selected as CPPs ionizable lipid proportion and type, buffer pH, and phospholipid content, while keeping the others constant based on the optimal settings underlined by the previous

screening. The new BBD was then performed using a more restricted range and fewer CPPs, and at the same time including additional CQAs such as protein expression, and cytokines expression by cells as endpoint for activation. In particular, higher pH demonstrated smaller particles size, while a higher amount of phospholipid resulted in larger size, higher EE and better RNA integrity. Higher ionizable lipid content improved the protein expression levels. Thus, the authors applied multiple desirability functions to find three hypothetical LNPs leads which they formulated and confirmed the model predictions, demonstrating high levels of protein expression, low cytokines productions, and desirable physio-chemical features. This study offers a very interesting framework for LNPs optimization, although it does not include any *in vivo* experiments that could have highly benefitted the translational relevance of this work.

Compared to other formulations, the production of LNPs involves many more CPPs, and their interactions can be very complex, making difficult to draw parallelisms among the studies mentioned above, other than generic extrapolation such as higher transfection requiring mostly higher percentages of ionizable lipids.

### 7.3. Biotechnological and biomimetic DDSs

DoE can also be applied to a variety of biotechnological production process to formulate biological and biomimetic nanovectors.

In the case of biological DDSs, a work by Puente-Massaguer et al. [54] focused on HIV Virus-Like Particles (VLPs) production conditions using the Sf9 cells expression system. The factors considered for optimization were the effect of cell concentration at infection (CCI), multiplicity of infection (MOI) and time of harvest (TOH). This study included as CQAs baculovirus infection, VLPs production, VLPs assembly, cell viability and VLPs productivity. These responses were combined to obtain an overall desirability function for the process optimization. The authors employed a BBD of 15 runs overall, considering two factor interactions and quadratic effects. The highest number of VLPs produced were with higher CCI and TOH, but at lower levels of MOI. On the other hand, VLPs assembly was decreased by longer TOH. After modeling, depending on the goal with the highest weight in the desirability function, either the number of produced VLPs or the highest encapsulation, two formulations were selected. The optimal conditions for the two different optimization goals resulted in the same CCI ( $3.7 \times 10^6$  cell/mL) and MOI (0.01) but different TOH were required, being 60 h post infection for the quality and 80 h post infection for the quantity objective. Both the optimal conditions were tested to generate two different VLPs formulations that validated the model, with results within the model predicted range, and with yields comparable to the gold standards processes. This study is especially relevant since it demonstrates how DoE can be applied efficiently not only to strictly technological and chemical settings, but also to biotechnologies and biological protocols.

The same authors applied a similar BBD 15 runs design to perform the optimization for the production of baculovirus NPs in High Five cells [55]. In this case the CPPs and CQAs were the same as before. The percentage of infection greatly increased with MOI and TOH but was negatively correlated with CCI. Other CPPs effects were analogous to previous studies. Authors applied again desirability functions to performed VLPs optimization. The authors validated the two optimum formulations which demonstrated highly improved VLPs production compared to traditional VLPs production methods, with high cell viability and NPs productivity.

Cell coating has been widely used as a biomimetic approach to improve NPs biocompatibility and circulation time. Red blood cells (RBCs) membrane coating represent the prototype of this strategy [56]. For instance, Mendes et al. [57] applied DoE to the optimization of RBCs-coated LNPs to improve the delivery of the model drugs atorvastatin and curcumin across the blood brain barrier (BBB). First the authors optimized LNPs formulation on their own, successfully translating them to their scalable homogenization-based production. Then, the

authors performed a Taguchi array to assess the effect of different volumes of RBCs vesicles, number of co-extrusions, and concentration of stearylamine used during extrusion to coat the LNPs, ultimately leading to small and stable RBCs-coated LNPs. Despite the wealth of data provided by this work, the authors did not perform any *in vitro* nor *in vivo* studies to validate the particles delivery across the BBB or therapeutic efficacy, and many decisions and NPs designs were performed following assumptions from the literature without validating them. These limitations severely hinder the therapeutic potential of this new nanovector.

Rampado et al. [58] focused on the optimization of biomimetic nanovesicles termed Leukosomes to improve the delivery of chemotherapeutics in colorectal cancer. Leukosomes are phospholipids and cholesterol-based nanovesicles functionalized by engrafting in their lipid bilayer membrane proteins derived from leukocytes. This functionalization allows Leukosomes to attain the same proprieties of the cells they are derived from, including avoidance of the reticulo-endothelial system (enabled by proteins such as CD45 and CD47) and adhere to inflamed endothelial cells (mediated by integrins). This platform has been applied successfully to many disease settings, including sepsis [59], inflammatory bowel disease [60], breast cancer and melanoma [61], and osteosarcoma [62]. In this instance, the authors applied the Nanoassemblr® microfluidic system for formulating and loading doxorubicin using a well-established remote loading approach. A BBD was employed to optimize the flow rate ratio between organic phase and aqueous phase containing the membrane proteins, the total flow rate in the system, and the weight ratio between membrane proteins and lipid components. The design elucidated that the FRR had a quadratic negative effect on particles size but a positive linear effect. Furthermore, increasing the amount of membrane proteins made the particles more negative, while the PDI was positively influenced by the TFR, FRR, and by their interaction effect. Overall, the optimized formulation was found to be one created using 1 mL/min TFR, 20:1 lipid: protein ratio, and an FFR of 4.88:1 (aqueous: ethanol phase). The particles demonstrated a suitable size of 150 nm, a PDI around 0.2, and a more negative zeta potential than similar liposomes. The leukosomes demonstrated good stability and a loading efficiency for doxorubicin around 90%. Furthermore, they retained the membrane proteins on their surface. These optimized leukosomes adhered to inflamed endothelial cells and macrophages more efficiently than liposomes, with comparable to slightly increased cytotoxic effects on colorectal cancer cells.

#### 7.4. Hybrid NPs-based DDSs

In some instances, different classes of materials can be combined to produce innovative DDSs.

Among these cases, Thanki et al. [63] optimized lipidoid-PLGA NPs to deliver siRNA against lung cancer. NPs were prepared using a double emulsion approach. The authors selected a three level 3<sup>2</sup> FFD to investigate the effect of two main CPPs (lipidoid content and lipidoid:siRNA ratio) on the particles CQAs, in this case size (<250 nm to ensure good cellular uptake), PDI < 0.3, a ZP > 0 mV to improve the adhesion to cells, EE >60%, high transfection efficiency (IC<sub>50</sub> below 5 nM), and low toxicity. Interestingly, higher Lipidoid:siRNA ratio reduced particles size and PDI, while the increase in lipidoid increased the ZP. Notably, EE was higher when both Lipidoid content and the ratio were both low or high at the same time. The transfection efficiency was proportional to Lipidoid content up to 15% content, while lower ratio was correlated with higher cell viability. The optimal operating space was defined based on the previously described cut-off values. A combination of settings within the experimental space was selected for further analysis using different lipid molecules. Of note, this new DDS showed superior transfection efficacy in silencing EGFR in lung cancer cells compared to DOTAP NPs and other lipidoid molecules, confirming suitable features as predicted by the model.

Similarly, Dormenval et al. [64] applied DoE to the optimization of freeze-drying for PLGA-lipidoid hybrid NPs for pulmonary siRNA

delivery. This study employed a first screening design to investigate the effect of device loading, feedstock concentration and outlet temperature on the features of the NPs. The authors set as desirable CQAs cut-offs final yield above 40%, the moisture content of the dried powder to be minimized, the median aerodynamic diameter between 1 and 5 µm, and the difference in size before and after freeze drying, to be minimized. After screening out the temperature from the first design due to lack of significance, a second smaller CCF design was performed to further optimize the powder features. The loading was measured in a narrower space within the range leading to acceptable particles sizes. The factors with largest effect on the response were the device loading increasing the size, and the stock concentration positively affecting the yield and particles diameter. The second DoE allowed thus to define a fraction of the experimental space with acceptable results. The optimal formulation selected for further studies demonstrated suitable features as predicted by the model and good *in vitro* activity in RAW 264.7 cells.

Another work following a very similar approach is offered by Lokras et al. [65] who studied Lipidoid-PLGA NPs to improve the delivery of anti-TNFα siRNA for pulmonary administration. The CQAs selected for the study were NPs size, PDI, ZP, EE, gene silencing and cell viability. Lipidoid content and lipidoid:siRNA ratio was selected as CPPs. The selected design was rotatable and demonstrated to have good predictive power for optimization. The authors applied this productive model to circumscribe a fraction of the design space that to achieve the desired QTPP (size = 220 nm, PDI < 0.3, ZP around 15-30 mV, EE > 60%, gene silencing as IC<sub>50</sub> < 25 nM and cell viability as IC<sub>50</sub> > 55 nM), but they did not select one specific formulation. The authors then applied an already optimized freeze dry procedure to obtain dry NPs powder with suitable size and morphology.

These lipidoid-polymer platforms can also be used to deliver different oligonucleotides such as antisense oligonucleotides (ASOs). In particular, Thanki et al. [66] focused on the optimization of PLGA-lipid NPs for ASO delivery prepared using a double emulsion approach. To this end, the authors focused on two main CPPs selected after a one-factor-at-a-time strategy: the amount of ionizable lipids (L5) and the L5 to ASO ratio. The selected CQAs were particles size (<300 nm), PDI (<0.3), ZP (≤ 30 mV), high encapsulation efficiency, high loading efficiency, high efficacy of Luc silencing in HeLa Cells, and low cell toxicity. These outputs were used to create a desirability function to enable optimization, leading to a set of formulations with 14–17% (w/w) L5 content and L5: Luc-ASO ratios from 11:1 to 21:1, which demonstrated improved silencing efficacy compared to reference NPs. A limitation of this study is the preliminary one-factor-at-a-time investigation, hindering the understanding of the process and could have been replaced by a screening design.

Hybrid materials can also be used to deliver small molecule drugs. Following this intuition, Ishak et al. [67] optimized lipid-polymer hybrid NPs (LPHNPs) formulated *via* nanoprecipitation to encapsulate and deliver Rutin (RU) across the BBB as an adjuvant compound against Alzheimer's Disease, thanks to its anti-oxidative effects and ability to interfere with amyloid fibrils formation [68]. This study applied a two-level FFD, considering as CPPs PLGA amount, lecithin/PLGA ratio, and Tween 80 concentration, each at two levels. The CQAs were the RU EE, the NPs size and their PDI. All three factors were found to significantly influence particles size and EE, while PDI was influenced only by PLGA amount. PLGA amount and w/w ratio both increased EE, and PLGA alone increased NPs size, while the ratio had a negative effect on NPs diameter. Tween 80 amount instead had a negative effect on these two CQAs. For the formulation's optimization, the desirability function was set to maximize EE, while particles size and PDI cutoffs were set as ≤250 nm and ≤ 0.3, respectively. Following this function, the optimal results obtained were PLGA amount, ratio, and Tween 80 concentration, equal to 75 mg, 3/1 and 0.5%, respectively. The predicted formulation was produced, demonstrating good accuracy of the predictions. The tested formulation demonstrated improved RU delivery to the brain in rat models, with similar efficacy to Tween 80, which is considered the

gold standard adjuvant for brain delivery thanks to its ability to bind ApoE *in vivo* and be directed across the BBB.

Meng et al. [69] instead focused on the optimization of Chitosan-PLGA NPs to improve the nasal delivery of the anti-Alzheimer drug Huperzine A, possibly reducing the systemic side effects that it can yield after its systemic administration. The NPs were produced using a solvent displacement approach and were functionalized with lactoferrin as active targeting moiety. The authors applied a BBD to optimize CPPs including polymer concentration, drug concentration and surfactant (polyvinyl alcohol, PVA) concentration. The CQAs were NPs size and EE. In line with previous studies, polymer concentration had a positive effect on EE, but drug concentration and surfactant concentration reduced the encapsulation. Drug and polymer amount increased the NPs size but the surfactant concentration reduced it. The optimal formulation was then calculated to have a polymer concentration of 6.13 mg/mL, a drug concentration of 12.98%, and a PVA concentration of 1.00 mg/100 mL, with predicted CQAs of 78.78% EE, and size of 120.94 nm, validating the model by formulating particles with this small size (150 nm) and high EE (73%). The particles showed good mucoadhesive properties, slow drug release *in vitro*, low cytotoxicity and good cellular uptake compared to non-functionalized NPs. Finally, the lactoferrin-functionalized particles were able to reach the brain of mice after nasal administration.

Other hybrid DDSs have been tested by Albano et al. [70] who focused on the optimization of lipid-polymer crystalline NPs to improve the delivery of the antitumor drug docetaxel, formulated using micro-emulsification complemented with sonication. The authors used an FFD 2<sup>3</sup> to screen for the effect of the concentration of poloxamer used as surfactant (poloxamer F68 and F127 used together in different ratios) and the concentration of the drug in the mixture, on particles CQAs (size, PDI, and ZP), with the specific to obtain NPs smaller than 250 nm in diameter and with a PDI <0.2. All the CPPs had a positive effect on size and PDI but the percentage of F127 negatively influenced the ZP. The authors circumscribed the most suitable experimental space and prepared two optimized NPs batches, each one using a single different surfactant. The optimized formulations showed a desirable small size and PDI, colloidal stability over 6 months, slow drug release, and crystalline structure. However, the authors gave no *in vitro* not *in vivo* evidence of their biocompatibility or antitumor efficacy.

Another work by Yacoub et al. [71] studied gelatin-PDLG polymer NPs prepared *via* emulsification to improve the retention of the arthritis medication piroxicam after intra-articular injection. The authors used a FFD considering as CPPs percentage of internal phase, percentage of gelatin and percentage of PDLG, and as CQAs particle size, PDI, mean dissolution time, the release rate constant, and the time needed for quarter and half of the drug payload to be released (T25% and T50%, respectively). The results showed that T25% was only positively influenced by gelatin concentration. T50% was influenced positively by the percentage of internal phase. The release rate constant was increased also by higher gelatin and higher internal phase fraction, and PDI was positively influenced only by gelatin percentage. However, the effect of CPPs on NPs size was not significant. Based on this model, one optimal formulation was selected, demonstrating low viscosity, good injectability and good *in vivo* efficacy in reducing cartilage erosion in arthritic rats.

### 7.5. Emulsions and suspensions-based DDSs to improve drugs pharmacokinetics

Several studies applying DoE focus on innovative way to formulate drugs as nanosuspensions or nanoemulsions with the aim of improving their bioavailability. Technically these systems are not DDSs by their traditional definition, that being particles encapsulating drugs and carrying them across biological barriers. However, these colloidal systems are still nano-sized and are still aimed at improving drugs pharmacokinetics, often by enabling their crossing of biological barriers through

alternative routes other than diffusion of cellular carriers, and therefore can still be considered nanovectors.

Among these formulations, a study by Mohammady et al. [72] focused on increasing the solubility of the beta-blocker drug carvedilol (CAR), by formulating it as a nano-co-crystal, improving its apparent solubility and bioavailability. This formulation was prepared using a sonication-based solvent displacement method. The authors employed a CCD to optimize three CPPs: CAR concentration, concentration of conformer (tartaric acid, TA) in the organic solution, the concentration of poloxamer-188 in the aqueous phase, and the water: organic phase ratio. CAR and poloxamer concentration proved to positively influence the particle size, while increasing the water:acetone ratio and TA concentration decreased it. Of note, two factors' interactions between CAR concentration and poloxamer concentration were also very relevant in defining the particles size. Two optimized formulations were selected from the screening to perform stability studies after lyophilization, proving that for both formulations a slow freezing protocol yielded a similar size to the original formulation. These optimized formulations also demonstrated very high CAR solubility suitable for the quick oral administration of CAR.

Nanosuspensions allow to administer a high dose of drugs and achieve fast release through the large surface offered by small drug clusters. Shekhawat et al. [73] focused on the optimization of nanosuspension formulation process to improve the solubility and bioavailability of the anti-hypertensive drug eprosartan mesylate (EM) *via* nanoprecipitation. To perform this, the authors applied a FCCCD following an RSM and considered three main CPPs chosen after performing FMEA: concentration of EM, concentration of the stabilizer (Soluplus®) and ultrasonication intensity. The main CQAs considered were the size and PDI of the particles forming the EM nanoemulsion. Intuitively, sonication amplitude reduced the particles size, while it had a small effect on the PDI. Similarly to other studies, increase in Soluplus® concentration gradually decreased both particles size and PDI and higher drug concentration resulted in larger size and PDI. After creating the RSM model, the optimized formulation with minimal size and PDI resulted to be 40% amplitude, 0.4% w/v of soluplus and 0.6% w/v of EM, with a size of 149 ± and PDI = 0.278 ± 0.004, and very fast release and high solubility compared to the free drug. This nanosuspension also demonstrated improved permeability in synthetic membranes and *ex vivo* intestinal tissues, achieving higher blood concentration after oral administration in mice.

Spray drying allows the formulation of NPs for multiple applications including pulmonary delivery. Munir et al. [74] optimized cationic RALA cell-penetrating peptide [75] functionalized DNA NPs as a dry powder to deliver DNA for pulmonary gene therapy prepared using spray-drying. The CPPs were mannitol concentration and inlet temperature, while the selected CQAs were the process yield, moisture content, NPs size, ZP, and EE. Increased mannitol was the only factor influencing product yield. However, mannitol had a negative effect on DNA EE. All CPPs influenced particles size, with less mannitol causing an increase in NPs size. Conversely, lower temperature and mannitol concentration led to higher ZP values. Minimal moisture was achieved at highest temperature and mannitol content. The optimized NPs had a temperature of 50 °C, spray rate of 80%, and spray frequency of 110 kHz. All the NPs features were in good accordance with model predictions. These particles demonstrated good transfection efficacy on lung carcinoma A549 cells at 2% and 3% mannitol concentration.

Another work focused on spray-drying is offered by Wei et al [76] who optimized the conditions for the production of model drug hesperidin nanocrystals from wet nanosuspensions with the aim to improve its solubility. The authors employed a first screening design including as CPPs the inlet temperature and feeding rate of spray dryer and the protectant (PVP), and using a CQAs only the particles size. The screening revealed that the amount of PVP protectant decreased particles size while temperature proportionally increased it. A second RSM design was created to minimize NPs size. The authors validated the method by

formulating nanocrystals using 5% (w/w) of PVP K25 and 18% (m/v) hesperidin nanosuspension, with an inlet temperature of 100 °C. These nanocrystals showed a crystalline structure with a small size (250 nm) and low PDI, high hesperidin solubility and faster release rate compared to the non-spray dried nanosuspensions. However, the authors did not give much information on the designs they used.

Traditional technologies have still been applied successfully to the formulation of these colloidal DDSs. For instance, Gieszinger et al. [77] produced PVA-stabilized NPs containing the antiepileptic drug lamotrigine (LAM) prepared by dry milling for nasal administration. The authors generated a FFD selecting as CPPs the milling time, milling speed, and the PVA:LAM ratio. The CQAs defined were NPs size and PDI, and the percentage of dissolved LAM from the samples after 5 and 10 min. These CQAs were defined according to the ICH Q8 guidelines for this specific pharmaceutical application, establishing a very well-defined QTPP. As discussed for similar processes, increasing milling time and speed decreased the NPs size and PDI. On the contrary, increasing these parameters also increased the release rate due to higher surface exposed by smaller particles, and increasing the PVA:LAM ratio also increased slightly the release rate. The authors applied a Monte Carlo simulation to select a small design space range and selected seven lead formulations, prepared progressively at lower levels of predicted robustness. All the NPs presented suitable size but only the most robust formulation had a very fast release, releasing all the drug after 10 min.

Another example is offered by Gajera et al. [78], who focused on the DoE-based optimization of a dried extrusion process to formulate cellulose-based nanosuspensions, aiming to improve the solubility and release profile of the antimycotic drug clotrimazole. The studies CPPs were the system inlet temperature, the feed rate, and the screw speed. The CQAs were the particles PDI and the moisture content, both to be minimized. The authors employed a BDD, revealing that higher temperature reduced the moisture content, while increased feed rate increased it. On the other hand, both higher temperature and feed rate increased the PDI. The authors formulated thus a desirability function and optimized the extrusion conditions using a temperature of 125 °C, a screw speed of 186 rpm, and a feed rate of 2.5 mL/min, with the optimized formulation in good agreement with model's prediction and showing a highly increased drug solubility and faster release in water and PBS.

Self-nano emulsifying drugs delivery systems (SNEDDSs) allow to improve the solubility and the absorption of hydrophobic drugs thanks to the high surface provided by small oil emulsified droplets [79]. A recent work by Shailendrakumar et al. [80] optimized a SNEDDS to increase the oral availability of pentoxifylline (PTX), a drug used for the treatment of intermittent claudication. In this case, the authors focused on the use of a MD to optimize the proportions of the self-emulsifying system components: namely, the oil (palm oil), the surfactant (Capmul® MCM), and co-surfactant (Tween 80). The design elucidated how it was intuitively possible to significantly reduce the size of the emulsified NPs by decreasing the amount of oil and increasing the proportions of surfactant and co-surfactant. This optimization resulted in 130 nm size, stable droplets with a slow release, and improved oral *in vivo* bioavailability in mice.

Another work from Schmied et al. [81] focused on the optimization of a SNEDDS of different poorly soluble drugs (celecoxib and fenofibrate). The authors applied a MD to establish a center point for the mixture of surfactant (Tween 80), oil phase (Mygliol 812), and cosolvent (Gelucire 44). From the center point the authors created an array of formulations equidistant from the center and organized as hexagon. The selected CQAs cutoffs were: droplet size < 50 nm, a PDI < 0.15, and a transmittance > 99% after dispersing the SNEDDS in water. After performing the first screening for each formulation, the authors manually circumscribed a smaller design space for further optimization, in some instances going slightly beyond the original design space. Statistical analysis revealed a complex profile of CPPs influence in all CQAs, including interactions and quadratic effects. In the case of celecoxib,

increasing Gelucire 44 decreased transmittance and emulsification grade. Mygliol 812 increased particles size and emulsification grade but had a more complex effect on the transmittance. On the other hand, Tween 80 concentration decreased particles concentration, increased transmittance, and decreased emulsification grade. Fenofibrate had a simpler profile, with higher Tween 80 decreasing particles size emulsification grade, and increasing transmittance. Increase in Mygliol 812 instead only caused a drop-in transmittance at high concentrations. The optimized SNEDDSs showed indeed suitable features and very quick drug release. However, the authors did not provide any evidence of *in vivo* bioavailability.

Nanoemulsions can also be used as DDSs for biological cargoes. For instance, Kramer et al. [82] focused on the optimization of a lyophilized nanoemulsion vaccine against *mycobacterium tuberculosis*. The authors first screened several potential excipients compatible with the tuberculosis MTB ID-93 antigen. After selecting few of them, the authors decided to employ three separate and parallel DoE approaches with different CPPs and CQAs. This strategy was chosen to reduce the overall experimental runs number. However, this choice appears to be not very efficient. Specifically, performing uncorrelated DoE screenings gave contrasting information about the most relevant CPPs and led to an increase in the number of potential lead formulations. It is unclear why the authors did not perform a more traditional low-resolution large screening including all the factors and screen the irrelevant ones out before performing a higher resolution design for optimization. In this way the data presented appears very fragmented and it is very difficult to gain a complete understanding of the process. Still, the authors were able to demonstrate that the candidate formulations were more stable than the liquid commercial vaccine formulation, retaining the same antigenicity but with longer antigen and colloidal stability in accelerated storage studies.

## 8. Conclusions: current limitations and future directions of DoE application in drug delivery

In this article, we gave overview of the main concepts of DoE and offered examples of the latest applications of DoE to nanovectors used for drug delivery. However, we would like to underline some of the more general shortcomings that affect many studies, to give a more critical understanding of DoE and point to new potential directions for improvement.

Firstly, in many cases the process that is being studied is not discussed extensively. When setting up a DoE for either screening and optimization, it can be very useful to contextualize the CPPs in study by presenting the entirety of the process as a cause-and-effect diagram, and by performing risk assessment on all the factors that are involved, stressing the decision-making process justifying why some CPPs have been selected over others. A good example of this is the previously discussed study by Shekhawat et al. [73], who applied the previously discussed FMEA approach.

Another limitation often found among these studies is the lack of information regarding the selected designs. Only seldomly the authors discuss the resolution of the design, its confounding properties, orthogonality of CPPs, number of replicates runs or replicate screenings, or the optimality of the design. This lack of definition of the design makes difficult to understand the validity of the results, and should be more often included in supporting material.

Furthermore, in most of the studies presented in this article, the number of experimental runs is limited to 15–20 runs per design. Such a low number of runs can limit the amount of information given by DoE. This is often caused by the intricacy of NPs production, and by the costs in terms of materials, time, and workforce. However, the practical limitations in NPs formulations could be overcome by using small-scale, high throughput techniques, including combinatorial screening approaches that allow to create tens of formulations in a short time, often through automation, or the use of commercially available instruments

specifically design for screening purposes. The combination of these techniques and DoE could potentially unlock an unprecedented amount of information on many different processes of NPs formulations. One such example is offered by Fan et al. [83] who used a robotic liquid handling solvent injection approach to prepare small volume of LNPs to deliver antisense oligonucleotides. This system allows to prepare hundreds of formulations per hour, and thus could exponentially increase the power of DoE-based screenings and optimization studies since allows to overcome the bottle neck posed by the experimental runs limit. In particular, this study used different N/P ratios, different overall lipid concentrations, and different PEG-lipid concentrations, with two separate ionizable and cationic lipids (MC3 and DOPTAP, respectively). The authors demonstrated how increasing PEGylated lipid proportion reduced particles size but increased their PDI, and to have EE above 80% it was necessary to have an N/P ratio above 1. This method demonstrated to be scalable to higher volumes, enabling the large-scale testing of lead formulations.

DoE allows us to investigate much more in-depth correlations between the experimental factors and the results. This is true especially for complex two or higher factors interactions. However, DoE does not provide *per se* any mechanistic information on what happens within the process. Thus, the uncovering of unexpected new correlations influencing the process in study *via* DoE could prime the investigation of the potential mechanisms underlying these correlations. Despite DoE strict mathematical rationale, it could be still potentially employed as a novel tool for mechanism discovery. DoE can also be applied in conjunction with machine learning and neural networks. These advanced data analysis approach allow to analyze systematically very large amounts of data in the literature [84]. This would allow the authors to understand which variables have already been widely investigated and which have not been analyzed as much or at all. This wider scope could unlock the analysis of unprecedented combinations of CPPs, potentially uncovering new interactions. Neural networks are also a tool to create more complex and accurate perdition models to interpolate DoE results [32] and relevant research effort is being undertaken in further applying intelligence to DDSs design [85].

Another important aspect observed in the reviewed literature is the application in many instances of DoE as a stand-alone strategy for variables screening and process optimization. However, in most cases the authors do not focus on a direct comparison with the state of the art. This juxtaposition could be applied to different stages of the design: the gold standard can be used as a starting point to create a design space around it to explore, to see if it can be improved upon, and at the same time using it as a center point in the design itself. On the other hand, the gold standard can be also used as a cutoff for optimization, allowing to specify the boundaries or the minimal acceptable performance that the new optimized formulations must surpass to be considered.

Perhaps the most critical limitation observed in many of the studies reviewed above is the limited relevance of the results by the small scope of the selected CQAs. Many studies perform screening and optimization of a nanopatform based exclusively on its physical attributes (Size, PDI, Zeta potential, Loading efficiency, release profile) or very limited biological evidence (*in vitro* studies on cell cultures). However, all these results and models correlate poorly with *in vivo* models. Thus, the relevance of a DoE-based studies could greatly benefit by adding more extensive *in vitro* readings such as nanoparticles uptake, or by using experimental models with better predictive profile. Furthermore, the inclusion of *in vivo* models for NPs absorption, biodistribution or targeting could greatly improve the impact of the study's results and could also be a source of unexpected correlations between CPPs and the biological behavior of NPs, prompting new insights as discussed above. A good example discussed above was given by Blakney *et al* [52], who utilized human skin explants models, providing very high translational potential to their work. Furthermore, the application of DoE so far has focused mostly on the optimization of NPs features to improve their efficacy. However, only a very small amount of works investigated on

the toxicological effects of NPs. Including more biocompatibility and safety CQAs could substantially increase the amount of information extracted from DoE-based studies.

Of note, many of the discussed studies also employ natural and naturally derived materials (e.g. chitosan, gelatin, alginate, amniotic fluid) [27,31,48] to prepare NPs. However, natural materials are often affected by intrinsic inter-batch variability caused by their composition and techniques of purification. Thus, including different material lots as NFs could highlight the relevance of batch-to-batch variability in the screening and optimization of DDSs. This issue is especially relevant in a perspective of process scaling up and robustness.

Finally, the majority of the cited study focus only on the small-scale production of DSS, but it would be of great relevance to also validate the findings of DoE by performing scaling up of the process, making the findings more relevant from a large-scale production perspective. The study from Nag et al. [45] is a good example of this approach.

In conclusion, we believe that the wide range of different processes analyzed and optimized using DoE is a testimony of the versatility of this strategy and these successes could prime the further expansion of its employment on new nanomaterials and DDSs.

### CRedit authorship contribution statement

**Riccardo Rampado:** Conceptualization, Data curation, Formal analysis, Investigation, Writing – original draft, Writing – review & editing. **Dan Peer:** Conceptualization, Data curation, Formal analysis, Funding acquisition, Writing – original draft, Writing – review & editing.

### Declaration of Competing Interest

D.P. declares the following competing financial interest(s): D.P. receives licensing fees (to patents on which he was an inventor) from, invested in, consults (or on scientific advisory boards or boards of directors) for, lectured (and received a fee) or conducts sponsored research at TAU for the following entities: ART Biosciences, BioNtech SE, Eleven Therapeutics, Kernal Biologics, Merck, Newphase Ltd., NeoVac Ltd., RiboX Therapeutics, Roche, SirTLabs Corporation, Teva Pharmaceutical Inc.

All other authors declare no competing financial interests.

### Data availability

No data was used for the research described in the article.

### Acknowledgements

This review is dedicated to Prof. Kinam Park for his years of devotion to research and his high standards that he implemented as Editor in Chief in the Journal of Controlled Release.

We would also like to thank Teva Pharmaceutical Industries Ltd. for sponsoring this work.

### References

- [1] NIST Sematech, *Engineering Statistics Handbook*, 2023.
- [2] Jiju Antony, *Design of Experiments for Engineers and Scientists*, Elsevier, 2014, <https://doi.org/10.1016/C2012-0-03558-2>.
- [3] B. Smucker, M. Krzywinski, N. Altman, *Optimal experimental design*, *Nat. Methods* 15 (2018) 559–560.
- [4] Z. Wu, W. Liu, W. Nie, *Literature review and prospect of the development and application of FMEA in manufacturing industry*, *Int. J. Adv. Manuf. Technol.* 112 (2021) 1409–1436.
- [5] Douglas C. Montgomery, *Design and Analysis of Experiments*, 8th edition, John Wiley & Sons, Incorporated, 2012.
- [6] *Handbook of Design and Analysis of Experiments*, Taylor & Francis Group, CRC Press, 2015.
- [7] R.M. Bruggen, *How to construct fractional factorial experiments*, *Technometrics* 34 (1992) 492–493.

- [8] Sør Bisgaard, Blocking generators for small  $2^{k-p}$  designs, *J. Qual. Technol.* 26 (1994) 288–296.
- [9] R.L. Plackett, J.P. Burman, The design of optimum multifactorial experiments, *Biometrika* 33 (1946) 305–325.
- [10] S. Bhattacharya, Central composite design for response surface methodology and its application in pharmacy, in: *Response Surface Methodology in Engineering Science*, IntechOpen, 2021, <https://doi.org/10.5772/intechopen.95835>.
- [11] G.E.P. Box, D.W. Behnken, Some new three level designs for the study of quantitative variables, *Technometrics* 2 (1960) 455.
- [12] R.N. Kacker, E.S. Lagergren, J.J. Filliben, Taguchi's orthogonal arrays are classical designs of experiments, *J. Res. Natl. Inst. Stand. Technol.* 96 (1991) 577.
- [13] Y.K. Sung, S.W. Kim, Recent advances in polymeric drug delivery systems, *Biomater. Res.* 24 (2020) 12.
- [14] H. Li, et al., Recent advances in development of dendritic <sc>polymer-based</sc> nanomedicines for cancer diagnosis, *WIREs Nanomed. Nanobiotechnol.* 13 (2021).
- [15] D. Essa, P.P.D. Kondiah, Y.E. Choonara, V. Pillay, The design of poly(lactide-co-glycolide) nanocarriers for medical applications, *Front. Bioeng. Biotechnol.* 8 (2020).
- [16] R. Gonzalez-Pizarro, et al., Development of fluorometholone-loaded PLGA nanoparticles for treatment of inflammatory disorders of anterior and posterior segments of the eye, *Int. J. Pharm.* 547 (2018) 338–346.
- [17] G.K. Jena, et al., QbD enabled optimization of solvent shifting method for fabrication of PLGA-based nanoparticles for promising delivery of Capecitabine for antitumor activity, *Drug Deliv. Transl. Res.* 12 (2022) 1521–1539.
- [18] R. Diwan, S. Khan, P.R. Ravi, Comparative study of cilnidipine loaded PLGA nanoparticles: process optimization by DoE, physico-chemical characterization and in vivo evaluation, *Drug Deliv. Transl. Res.* 10 (2020) 1442–1458.
- [19] G. Esteruelas, et al., Development and optimization of Riluzole-loaded biodegradable nanoparticles incorporated in a mucoadhesive in situ gel for the posterior eye segment, *Int. J. Pharm.* 612 (2022), 121379.
- [20] R. Diwan, P.R. Ravi, S.I. Agarwal, V. Aggarwal, Cilnidipine loaded poly( $\epsilon$ -caprolactone) nanoparticles for enhanced oral delivery: optimization using DoE, physical characterization, pharmacokinetic, and pharmacodynamic evaluation, *Pharm. Dev. Technol.* 26 (2021) 278–290.
- [21] H. Vardhan, P. Mittal, S.K.R. Adena, M. Upadhyay, B. Mishra, Development of long-circulating docetaxel loaded poly(3-hydroxybutyrate-co-3-hydroxyvalerate) nanoparticles: optimization, pharmacokinetic, cytotoxicity and in vivo assessments, *Int. J. Biol. Macromol.* 103 (2017) 791–801.
- [22] X. Yu, et al., Zein nanoparticles as nontoxic delivery system for maytansine in the treatment of non-small cell lung cancer, *Drug Deliv.* 27 (2020) 100–109.
- [23] C. Webb, et al., Using microfluidics for scalable manufacturing of nanomedicines from bench to GMP: a case study using protein-loaded liposomes, *Int. J. Pharm.* 582 (2020), 119266.
- [24] E. Chiesa, R. Dorati, T. Modena, B. Conti, I. Genta, Multivariate analysis for the optimization of microfluidics-assisted nanoprecipitation method intended for the loading of small hydrophilic drugs into PLGA nanoparticles, *Int. J. Pharm.* 536 (2018) 165–177.
- [25] S.G. Pinar, H. Canpinar, Ç. Tan, N. Çelebi, A new nanosuspension prepared with wet milling method for oral delivery of highly variable drug cyclosporine a: development, optimization and in vivo evaluation, *Eur. J. Pharm. Sci.* 171 (2022), 106123.
- [26] P. Calvo, C. Remuán-López, J.L. Vila-Jato, M.J. Alonso, Chitosan and chitosan/ethylene oxide-propylene oxide block copolymer nanoparticles as novel carriers for proteins and vaccines, *Pharm. Res.* 14 (1997) 1431–1436.
- [27] J. Shailender, P.R. Ravi, M. Reddy Sirukuri, A. Dalvi, O. Keerthi Priya, Chitosan nanoparticles for the oral delivery of tenofovir disoproxil fumarate: formulation optimization, characterization and ex vivo and in vivo evaluation for uptake mechanism in rats, *Drug Dev. Ind. Pharm.* 44 (2018) 1109–1119.
- [28] M. Baghaei, et al., Optimization of chitosan-based polyelectrolyte nanoparticles for gene delivery, using design of experiment: in vitro and in vivo study, *Mater. Sci. Eng. C Mater. Biol. Appl.* 118 (2021), 111036.
- [29] S. Yadav, J. Singhal, S.S. Singhal, S. Awasthi, hSET1: A novel approach for colon cancer therapy, *Biochem. Pharmacol.* 77 (2009) 1635–1641.
- [30] B. von Storp, A. Engel, A. Boeker, M. Ploeger, K. Langer, Albumin nanoparticles with predictable size by desolvation procedure, *J. Microencapsul.* 29 (2012) 138–146.
- [31] H. Abdelrady, R.M. Hathout, R. Osman, I. Saleem, N.D. Mortada, Exploiting gelatin nanocarriers in the pulmonary delivery of methotrexate for lung cancer therapy, *Eur. J. Pharm. Sci.* 133 (2019) 115–126.
- [32] A.E. Koletti, et al., Gelatin nanoparticles for NSAID systemic administration: quality by design and artificial neural networks implementation, *Int. J. Pharm.* 578 (2020), 119118.
- [33] L. Xu, et al., Lipid nanoparticles for drug delivery, *Adv. Nanobiomed. Res.* 2 (2022) 2100109.
- [34] R.B. Rigon, et al., Solid lipid nanoparticles optimized by 22 factorial design for skin administration: cytotoxicity in NIH3T3 fibroblasts, *Colloids Surf. B: Biointerfaces* 171 (2018) 501–505.
- [35] N. Chokshi, v. Khatri, H. N. & Patel, M. M., Formulation, optimization, and characterization of rifampicin-loaded solid lipid nanoparticles for the treatment of tuberculosis, *Drug Dev. Ind. Pharm.* 44 (2018) 1975–1989.
- [36] S. Pandey, P. Patel, A. Gupta, Novel solid lipid nanocarrier of glibenclamide: a factorial design approach with response surface methodology, *Curr. Pharm. Des.* 24 (2018) 1811–1820.
- [37] N. Kumar, S. Goindi, Development and optimization of itraconazole-loaded solid lipid nanoparticles for topical administration using high shear homogenization process by design of experiments: in vitro, ex vivo and in vivo evaluation, *AAAPS PharmSciTech* 22 (2021) 248.
- [38] N.R. Rarokar, P.B. Khedekar, A.P. Bharne, M.J. Umekar, Development of self-assembled nanocarriers to enhance antitumor efficacy of docetaxel trihydrate in MDA-MB-231 cell line, *Int. J. Biol. Macromol.* 125 (2019) 1056–1068.
- [39] A.M. Nazief, P.S. Hassaan, H.M. Khalifa, M.S. Sokar, A.H. El-Kamel, Lipid-based gliclazide nanoparticles for treatment of diabetes: formulation, pharmacokinetics, pharmacodynamics and subacute toxicity study, *Int. J. Nanomedicine* 15 (2020) 1129–1148.
- [40] R. Diwan, P.R. Ravi, N.S. Pathare, V. Aggarwal, Pharmacodynamic, pharmacokinetic and physical characterization of cilnidipine loaded solid lipid nanoparticles for oral delivery optimized using the principles of design of experiments, *Colloids Surf. B: Biointerfaces* 193 (2020), 111073.
- [41] G.M. Patel, P.K. Shelat, A.N. Lalwani, QbD based development of proliposome of lopinavir for improved oral bioavailability, *Eur. J. Pharm. Sci.* 108 (2017) 50–61.
- [42] R. Mashima, S. Takada, Lipid nanoparticles: a novel gene delivery technique for clinical application, *Curr. Issues Mol. Biol.* 44 (2022) 5013–5027.
- [43] S. Yonezawa, H. Koide, T. Asai, Recent advances in siRNA delivery mediated by lipid-based nanoparticles, *Adv. Drug Deliv. Rev.* 154–155 (2020) 64–78.
- [44] X. Hou, T. Zaks, R. Langer, Y. Dong, Lipid nanoparticles for mRNA delivery, *Nat. Rev. Mater.* 6 (2021) 1078–1094.
- [45] K. Nag, et al., DoE-derived continuous and robust process for manufacturing of pharmaceutical-grade wide-range LNPs for RNA-vaccine/drug delivery, *Sci. Rep.* 12 (2022) 9394.
- [46] M. Danaei, et al., Impact of particle size and polydispersity index on the clinical applications of lipidic nanocarrier systems, *Pharmaceutics* 10 (2018) 57.
- [47] K.J. Hassett, et al., Impact of lipid nanoparticle size on mRNA vaccine immunogenicity, *J. Control. Release* 335 (2021) 237–246.
- [48] K.L. Swingle, et al., Amniotic fluid stabilized lipid nanoparticles for in utero intra-amniotic mRNA delivery, *J. Control. Release* 341 (2022) 616–633.
- [49] A. Hashiba, et al., The use of design of experiments with multiple responses to determine optimal formulations for in vivo hepatic mRNA delivery, *J. Control. Release* 327 (2020) 467–476.
- [50] M.M. Billingsley, et al., Orthogonal design of experiments for optimization of lipid nanoparticles for mRNA engineering of CAR T cells, *Nano Lett.* 22 (2022) 533–542.
- [51] K. Bloom, F. van den Berg, P. Arbutnot, Self-amplifying RNA vaccines for infectious diseases, *Gene Ther.* 28 (2021) 117–129.
- [52] A.K. Blakney, et al., The skin you are in: design-of-experiments optimization of lipid nanoparticle self-amplifying RNA formulations in human skin explants, *ACS Nano* 13 (2019) 5920–5930.
- [53] H.H. Ly, S. Daniel, S.K. Soriano, v. Kis, Z. & Blakney, A. K., Optimization of lipid nanoparticles for saRNA expression and cellular activation using a design-of-experiment approach, *Mol. Pharm.* 19 (2022) 1892–1905.
- [54] E. Puente-Massaguer, M. Lecina, F. Gódia, Application of advanced quantification techniques in nanoparticle-based vaccine development with the SF9 cell baculovirus expression system, *Vaccine* 38 (2020) 1849–1859.
- [55] E. Puente-Massaguer, M. Lecina, F. Gódia, Integrating nanoparticle quantification and statistical design of experiments for efficient HIV-1 virus-like particle production in high five cells, *Appl. Microbiol. Biotechnol.* 104 (2020) 1569–1582.
- [56] R. Rampado, P. Caliceti, M. Agostini, Latest advances in biomimetic cell membrane-coated and membrane-derived nanovectors for biomedical applications, *Nanomaterials* 12 (2022) 1543.
- [57] M. Mendes, et al., Biomimetic ultra-small lipid nanoconstructs for glioblastoma treatment: a computationally guided experimental approach, *Int. J. Pharm.* 587 (2020), 119661.
- [58] R. Rampado, et al., Optimization of biomimetic, leukocyte-mimicking nanovesicles for drug delivery against colorectal cancer using a design of experiment approach, *Front. Bioeng. Biotechnol.* 10 (2022).
- [59] R. Molinaro, et al., Macrophage-derived nanovesicles exert intrinsic anti-inflammatory properties and prolong survival in sepsis through a direct interaction with macrophages, *Nanoscale* 11 (2019) 13576–13586.
- [60] R. Molinaro, et al., Design and development of biomimetic nanovesicles using a microfluidic approach, *Adv. Mater.* 30 (2018) 1702749.
- [61] R. Molinaro, et al., Leukocyte-mimicking nanovesicles for effective doxorubicin delivery to treat breast cancer and melanoma, *Biomater. Sci.* 8 (2020) 333–341.
- [62] F. Giordano, et al., Tyrosine kinase inhibitor-loaded biomimetic nanoparticles as a treatment for osteosarcoma, *Cancer Nanotechnol.* 13 (2022) 40.
- [63] K. Thanki, et al., Engineering of small interfering RNA-loaded lipidoid-poly(DL-lactic-co-glycolic acid) hybrid nanoparticles for highly efficient and safe gene silencing: A quality by design-based approach, *Eur. J. Pharm. Biopharm.* 120 (2017) 22–33.
- [64] C. Dormenval, et al., Identification of factors of importance for spray drying of small interfering RNA-loaded Lipidoid-polymer hybrid nanoparticles for inhalation, *Pharm. Res.* 36 (2019) 142.
- [65] A. Lokras, C. Foged, A. Thakur, Engineering of solid dosage forms of siRNA-loaded lipidoid-polymer hybrid nanoparticles using a quality-by-design approach, *Methods Mol. Biol.* 2282 (2021) 137–157.
- [66] K. Thanki, et al., Application of a quality-by-design approach to optimise lipid-polymer hybrid nanoparticles loaded with a splice-correction antisense oligonucleotide: maximising loading and intracellular delivery, *Pharm. Res.* 36 (2019) 37.
- [67] R.A.H. Ishak, N.M. Mostafa, A.O. Kamel, Stealth lipid polymer hybrid nanoparticles loaded with rutin for effective brain delivery - comparative study with the gold standard (Tween 80): optimization, characterization and biodistribution, *Drug Deliv.* 24 (2017) 1874–1890.

- [68] S. Habtemariam, Rutin as a natural therapy for Alzheimer's disease: insights into its mechanisms of action, *Curr. Med. Chem.* 23 (2016) 860–873.
- [69] Q. Meng, et al., Intranasal delivery of Huperzine A to the brain using lactoferrin-conjugated N-trimethylated chitosan surface-modified PLGA nanoparticles for treatment of Alzheimer's disease, *Int. J. Nanomedicine* 13 (2018) 705–718.
- [70] J.M.R. Albano, et al., Rational design of polymer-lipid nanoparticles for docetaxel delivery, *Colloids Surf. B: Biointerfaces* 175 (2019) 56–64.
- [71] A.S. Yacoub, H.O. Ammar, M. Ibrahim, S.M. Mansour, N.M. el Hoffy, Artificial intelligence-assisted development of in situ forming nanoparticles for arthritis therapy via intra-articular delivery, *Drug Deliv.* 29 (2022) 1423–1436.
- [72] M. Mohammady, M. Hadidi, S. Iman Ghetmiri, G. Yousefi, Design of ultra-fine carvedilol nanocrystals: development of a safe and stable injectable formulation, *Eur. J. Pharm. Biopharm.* 168 (2021) 139–151.
- [73] P. Shekhawat, V. Pokharkar, Risk assessment and QbD based optimization of an Eprosartan mesylate nanosuspension: in-vitro characterization, PAMPA and in-vivo assessment, *Int. J. Pharm.* 567 (2019), 118415.
- [74] M. Munir, V.L. Kett, N.J. Dunne, H.O. McCarthy, Development of a spray-dried formulation of peptide-DNA nanoparticles into a dry powder for pulmonary delivery using factorial design, *Pharm. Res.* 39 (2022) 1215–1232.
- [75] Y. Liu, et al., Development and characterization of high efficacy cell-penetrating peptide via modulation of the histidine and arginine ratio for gene therapy, *Materials* 14 (2021) 4674.
- [76] Q. Wei, C.M. Keck, R.H. Müller, Solidification of hesperidin nanosuspension by spray drying optimized by design of experiment (DoE), *Drug Dev. Ind. Pharm.* 44 (2018) 1–12.
- [77] P. Giesinger, et al., Definition and validation of the design space for co-milled nasal powder containing nanosized lamotrigine, *Drug Dev. Ind. Pharm.* 44 (2018) 1622–1630.
- [78] B.Y. Gajera, D.A. Shah, R.H. Dave, Investigating a novel hot melt extrusion-based drying technique to solidify an amorphous nanosuspension using design of experiment methodology, *AAPS PharmSciTech* 19 (2018) 3778–3790.
- [79] D. Singh, Self-nanoemulsifying drug delivery system: a versatile carrier for lipophilic drugs, *Pharm. Nanotechnol.* 9 (2021) 166–176.
- [80] A.M. Shailendrakumar, V.M. Ghate, M. Kinra, S.A. Lewis, Improved oral pharmacokinetics of pentoxifylline with palm oil and Capmul® MCM containing self-nano-emulsifying drug delivery system, *AAPS PharmSciTech* 21 (2020) 118.
- [81] F.-P. Schmied, A. Bernhardt, A. Engel, S. Klein, A customized screening tool approach for the development of a self-nanoemulsifying drug delivery system (SNEDDS), *AAPS PharmSciTech* 23 (2021) 39.
- [82] R.M. Kramer, et al., Development of a thermostable nanoemulsion adjuvanted vaccine against tuberculosis using a design-of-experiments approach, *Int. J. Nanomedicine* 13 (2018) 3689–3711.
- [83] Y. Fan, et al., Automated high-throughput preparation and characterization of oligonucleotide-loaded lipid nanoparticles, *Int. J. Pharm.* 599 (2021), 120392.
- [84] Z. Ban, Q. Zhou, A. Sun, L. Mu, X. Hu, Screening priority factors determining and predicting the reproductive toxicity of various nanoparticles, *Environ. Sci. Technol.* 52 (2018) 9666–9676.
- [85] P. Tan, X. Chen, H. Zhang, Q. Wei, K. Luo, Artificial intelligence aids in development of nanomedicines for cancer management, *Semin. Cancer Biol.* 89 (2023) 61–75.